Experimental Supporting Information for:

Testing the Push-Pull Hypothesis: Lewis-Acid Augmented N_2 Activation

Jacob B. Geri, James Shanahan, Nathaniel K. Szymczak*

Department of Chemistry, University of Michigan, 930 North University Avenue, Ann Arbor, MI 48109, United States

Table of Contents

General Considerations:

Throughout the supporting information and main text, tetrakis(3,5-bistrifluoromethylphenyl)borate and tetrakis(pentafluorophenyl)borate are abbreviated as $BAr^F{}_4$ and $B(C_6F_5)_4^-$, respectively. $B(C_6F_5)$, $B(C_6H_5)_3$, $Li(Et_2O)(B(C_6F_5)_4)$, $Fe(Cp^*)_2$, $BF_3{\bullet}OEt_2$, 1,2-bis(diethylphosphino)ethane (depe), and iron dichloride were used from commercial sources without further purification. $^{15}N_2$ (98%) was purchased from Cambridge Isotope Laboratories. Tetrahydrofuran, pentane, and diethyl ether were purified using a Glass Contour solvent purification system through percolation through a Cu catalyst, molecular sieves, and alumina and finally stored over activated molecular sieves for a minimum of 48 hours, then stored over potassium mirrors. Toluene, benzene, and methyl tert-butyl ether were distilled from molten sodium/ketyl radical and stored over potassium mirrors. Fluorobenzene was fractionally distilled from P_2O_5 after stirring for three days. Diisopropyl ketone was distilled from calcium hydride and stored over molecular sieves. Fe(II)(^{i}Pr$_2$Tp)Cl,[1] $Fe(depe)_2N_2$,[2] $NaBAr^F{}_4$,[3] $KBAr^F{}_4$, $RbBAr^F{}_4$, $CsBAr^F{}_4$,[4] $H(OEt_2)_2BAr^F{}_4$,[5] $B(C_6H_3F_2)_3$, $B(C_6H_2F_3)_3$,[6] and $B(OC_6F_5)_3$[7] were prepared according to literature methods. Tetrabutylammonium $BAr^F{}_4$ was prepared according to literature methods, doubly recrystallized, then dried over P_2O_5 for three days under high vacuum.[8] Unless otherwise specified, all reactions were prepared and carried out in an anhydrous nitrogen atmosphere using standard Schlenk and/or glovebox techniques.

NMR spectra were recorded on a Varian Vnmrs 700, Varian Inova 500, or Varian MR400 spectrometer. ^{1}H, ^{13}C, ^{15}N, ^{19}F, ^{11}B, and ^{31}P shifts are reported in parts per million (ppm) relative to TMS, with the residual solvent peak used as an internal reference. ^{31}P, ^{15}N, ^{11}B, and ^{19}F NMR spectra are referenced on a unified scale, where the single primary reference is the frequency of the residual solvent peak in the ^{1}H NMR spectrum. Multiplicities are reported as follows: singlet (s), doublet (d), triplet (t), quartet (q), and multiplet (m). Transmission IR spectra were recorded on a Nicolet iS10 using either a bolt KBr press or 0.25 mm path length KBr solution cell, and electronic absorption spectra were recorded on a Varian Cary-50 spectrophotometer. Crystals were mounted on a Rigaku AFC10K Saturn 944+ CCD-based X-ray diffractometer equipped with a low temperature device and Micromax-007HF Cu-target micro-focus rotating anode (λ = 1.54187 Å) operated at 1.2 kW power (40 kV, 30 mA). The X-ray intensities were measured at 85(1) K with the detector placed at a distance 42.00 mm from the crystal; the data were processed with CrystalClear 2.011 and corrected for absorption. The structures were solved and refined with the Olex2 software package[9] and ShelXL.[10]

Syntheses

Fe(depe)$_2$(μ-N$_2$)(B(C$_6$F$_5$)$_3$) (2):

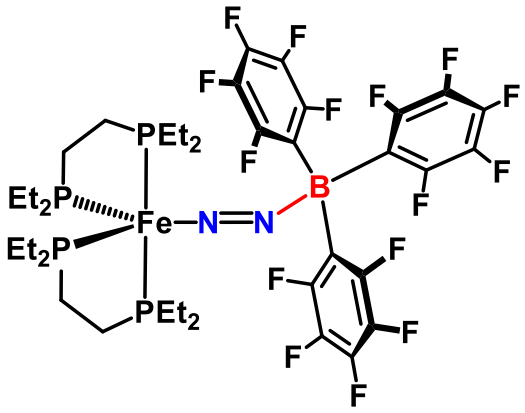

Fe(depe)$_2$N$_2$ (**1**) (25.0 mg, 50.0 μmol) and B(C$_6$F$_5$)$_3$ (25.8 mg, 50.0 μmol) were combined in a scintillation vial. Pentane (4 mL) was then added at room temperature and the mixture stirred for three minutes, generating a dark brown precipitate. The solvent was then removed under vacuum and the residual crystals washed with pentane (1 mL). This pentane was then removed by syringe and the solid dried under vacuum for 10 minutes to afford Fe(depe)$_2$(μ-N$_2$)(B(C$_6$F$_5$)$_3$) (**2**) (44.3 mg, 87% yield) as black crystals. A C$_6$D$_6$ solution of **2** was used for transmission IR spectroscopy. ^{1}H-NMR (C$_6$D$_6$): 1.42 (-C*H*$_2$, 2H, m), 1.35 (-C*H*$_2$, 2H, m), 1.20 (-C*H*$_2$, 2H, m), 1.13 (-C*H*$_2$, 2H, m), 1.11 (-C*H*$_2$, 2H, m), 0.82 (-C*H*$_3$, 6H, broad), 0.75 (-C*H*$_2$, 2H, m), 0.56 (-C*H*$_3$, 6H, m). ^{19}F-NMR (C$_6$D$_6$): -131.65 (-*o* F, 6F, d ($J_{19F\text{-}19F}$=19.1)), -159.47 (-*p* F, 3F, t ($J_{19F\text{-}19F}$=20.8)), -164.83 (-*m* F, 6F, t ($J_{19F\text{-}19F}$=19.2)). ^{11}B-NMR (C$_6$D$_6$): -6.35 (s). ^{31}P-NMR (C$_6$D$_6$): 76.15 (s). ^{15}N-NMR ((C$_6$H$_5$F): -10.54 (1N, s), -119.83 (1N, s). IR (C$_6$D$_6$, cm^{-1}): ^{14}N-^{14}N: 1816.3, ^{15}N-^{15}N: 1757.9 (calc.: 1753.6). **2** can be prepared in-situ through combining a 1:1 ratio of Fe(depe)$_2$N$_2$ with B(C$_6$F$_5$)$_3$ in a variety of solvents (IR, cm^{-1}): C$_6$D$_6$: 1816.3, PhF: 1810.3, methyl tert-butyl ether: 1816.6, tetrahydrofuran: 1805.0.

Fe(depe)$_2$(μ-^{15}N$_2$)(B(C$_6$F$_5$)$_3$) (2-^{15}N):

1 (5.0 mg, 10 μmol) was dissolved in C$_6$D$_6$ (500 μL) in a screw-cap scintillation vial. 4 mL ^{15}N$_2$ was sparged through the solution, and the solution allowed to stand for five days. Solid B(C$_6$F$_5$)$_3$ (5.2 mg, 10 μmol) was then added, and the resulting solution was analyzed by transmission IR spectroscopy. For ^{15}N-NMR characterization, **1** (5.0 mg, 10 μmol) was dissolved in C$_6$H$_5$F (500 μL) in a screw-cap NMR tube under an argon atmosphere. Solid B(C$_6$F$_5$)$_3$ (5.2 mg, 10 μmol) was then added, and the tube inverted until homogeneous (<1 minute). 3 mL ^{15}N$_2$ was sparged through the solution, and the solution allowed to stand for three minutes, and then immediately analyzed by ^{15}N-NMR.

Fig. ES1. ^{1}H NMR Spectrum and Aliphatic Region Detail:

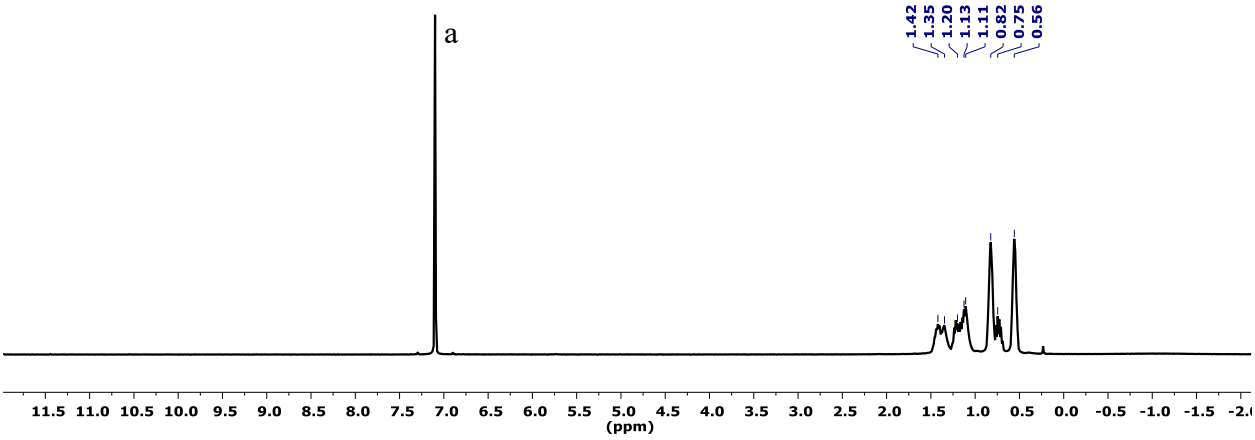

a: C_6H_6

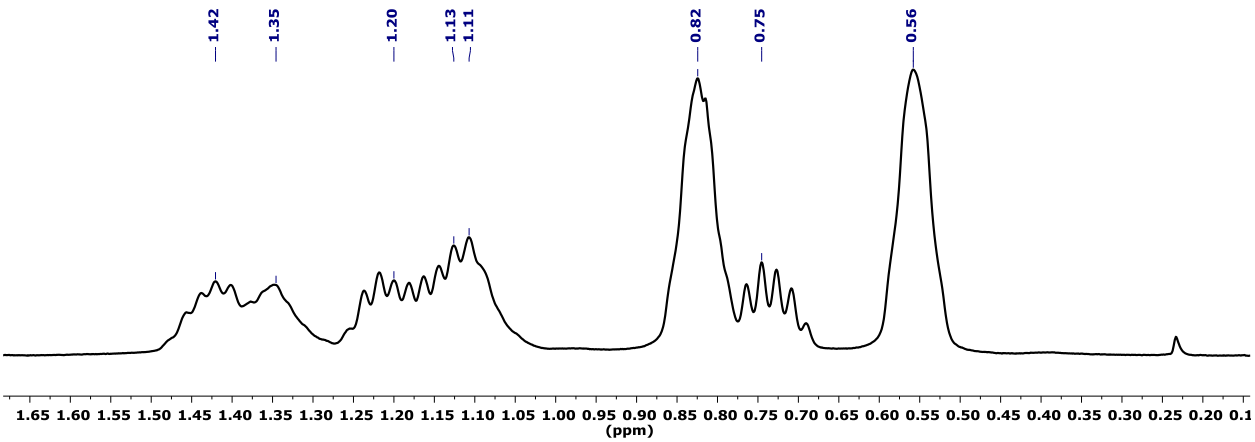

Fig. ES2. ^{19}F NMR Spectrum:

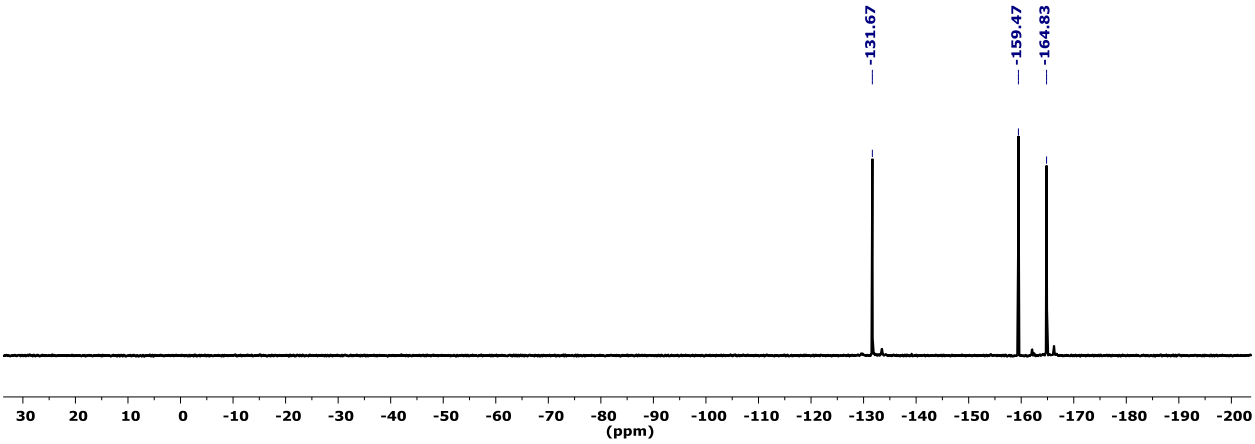

Fig. ES3. ^{11}B NMR Spectrum:

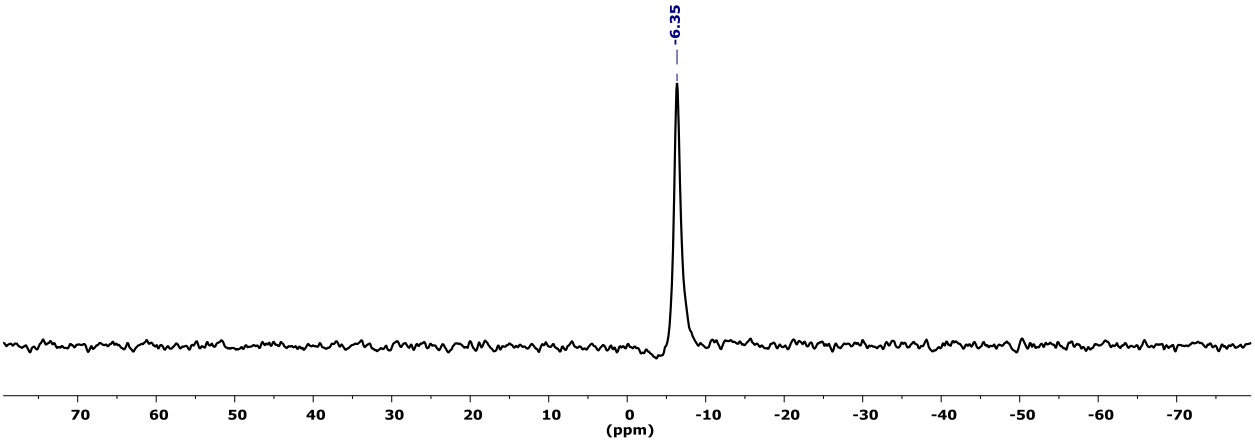

Fig. ES4. ^{31}P NMR Spectrum:

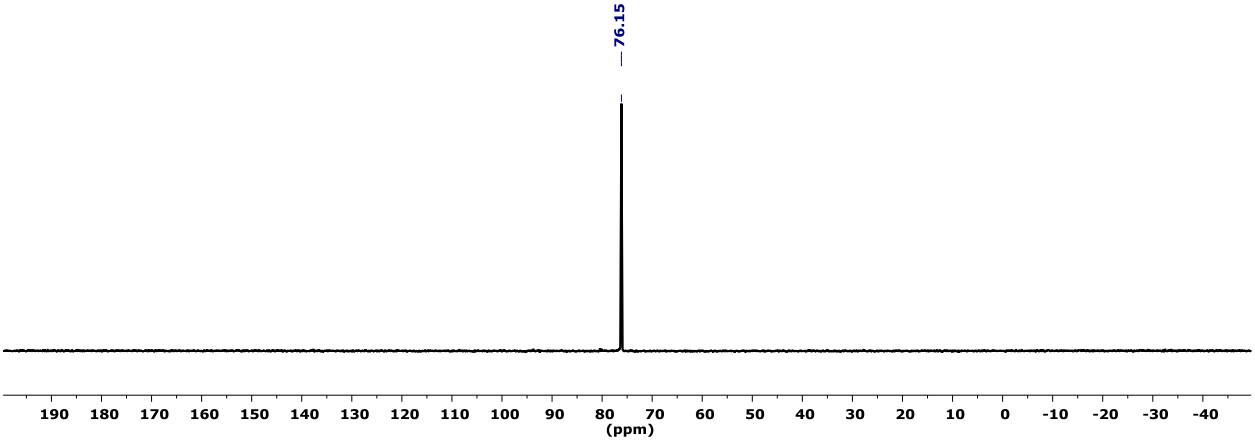

Fig. ES5. ^{15}N NMR Spectrum:

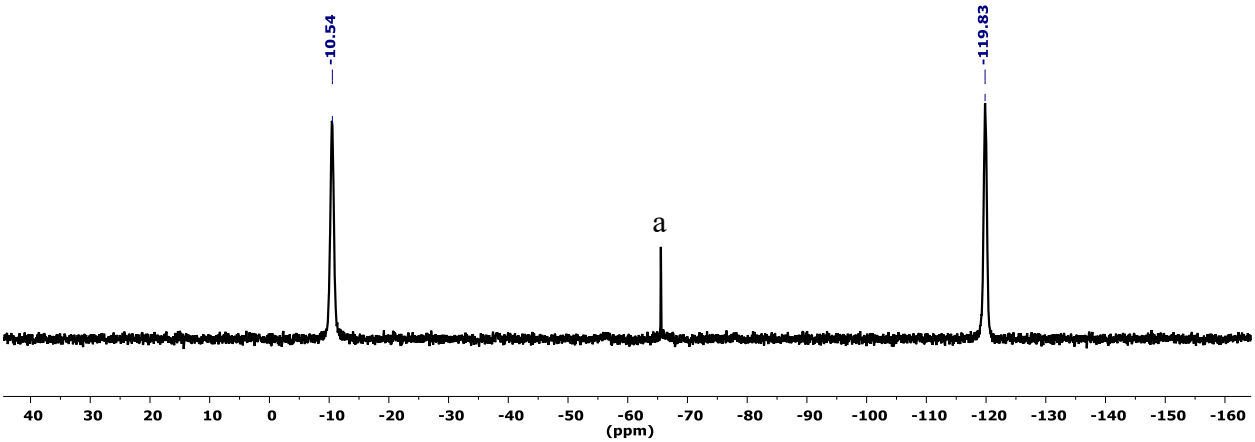

a: $^{15}N_2$

Fig. ES6. ^{1}H-^{13}C gHSQC Spectrum:

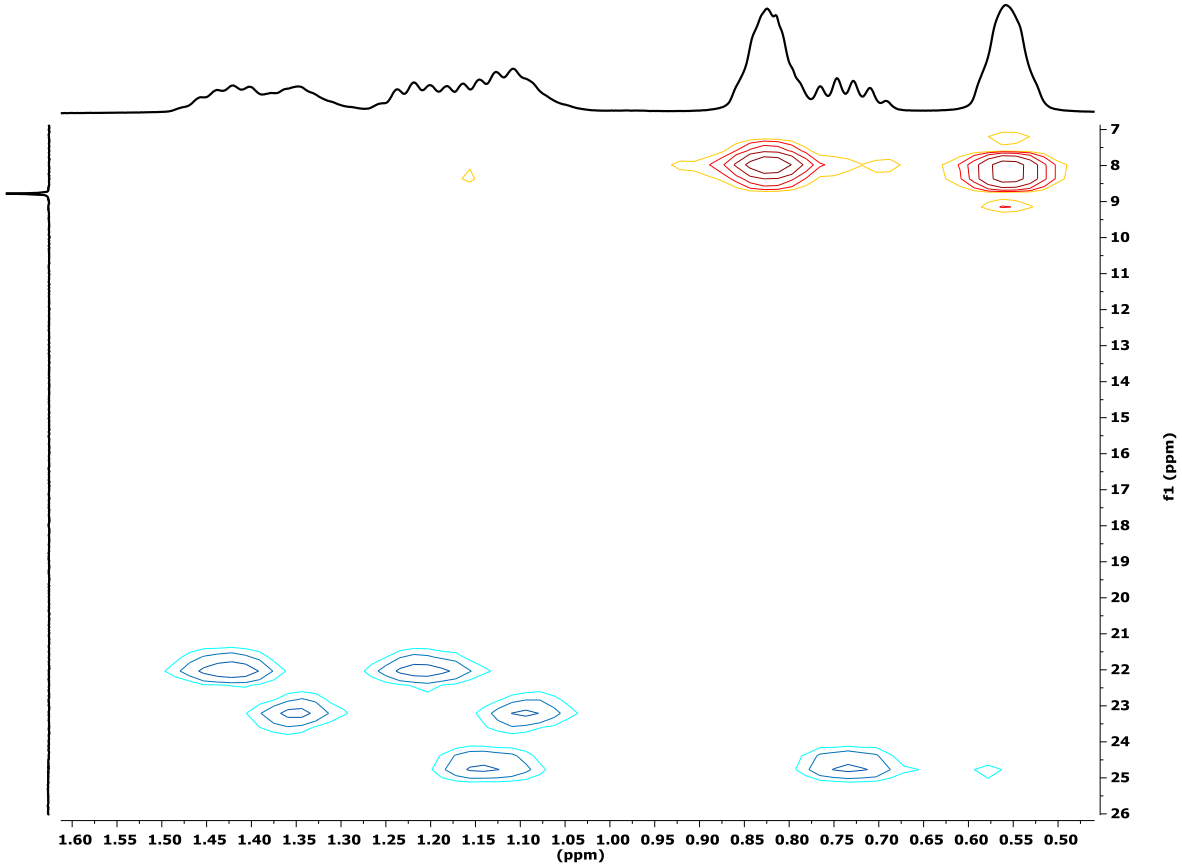

Fig. ES7. IR Spectrum:

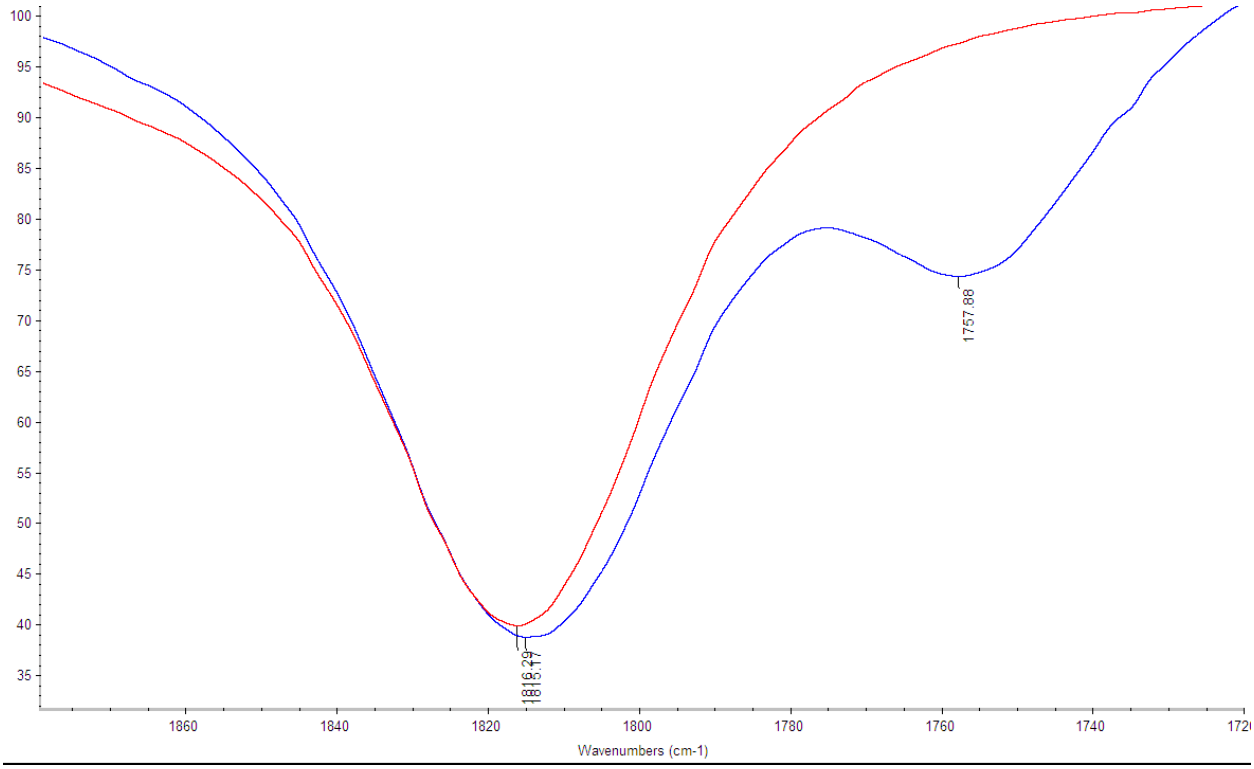

Blue: $^{15}N_2$-labeled $Fe(depe)_2(\mu\text{-}N_2)(B(C_6F_5)_3)$. Red: $^{14}N_2$- $Fe(depe)_2(\mu\text{-}N_2)(B(C_6F_5)_3)$.

Fig. ES8. X-Ray Crystal Structure:

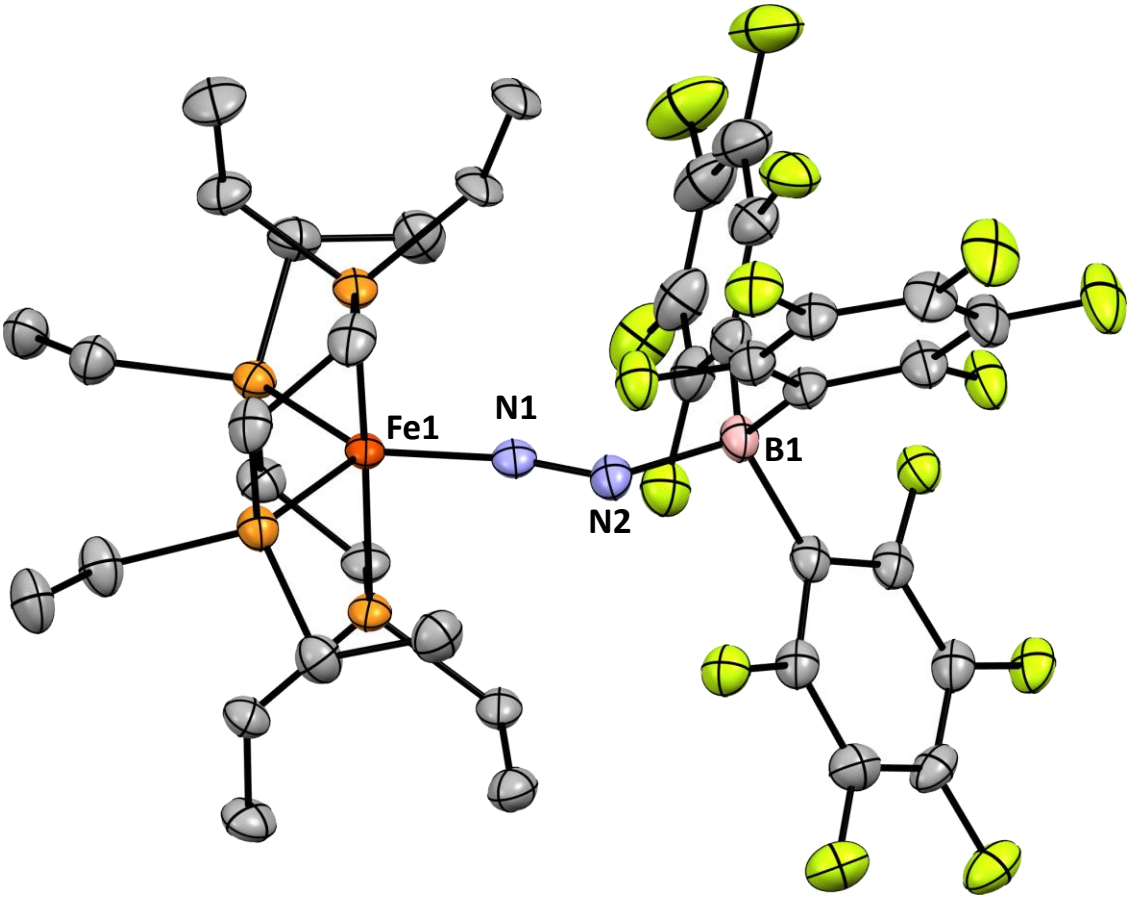

N1-N2: 1.18 Å; Fe1-N1: 1.71 Å; B1-N2-N1: 137 °

Fe(depe)$_2$(μ-N$_2$H)(B(C$_6$F$_5$)$_3$)(BAr$^F{}_4$) (3):

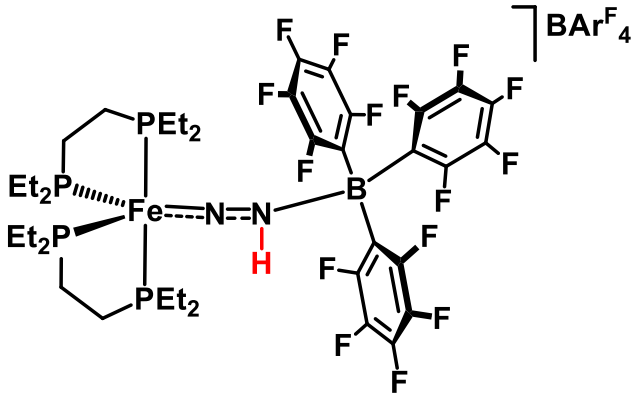

A solution of **2** (50 μmol in 4.0 mL C$_6$H$_5$F, 12.5 mM) was cooled to -30 °C in a small scintillation vial containing a teflon-coated stirbar. H(OEt$_2$)$_2$BAr$^F{}_4$ (50.6 mg, 50 μmol) was rapidly added to **2** in one portion, and vigorously shaken for 10 seconds to provide a homogeneous solution. The deep red solution of **2** immediately changes to an intense purple. The solution was then layered with 15 mL of -30 °C pentane and allowed to stand overnight, affording large purple crystals. The solvent was decanted, the crystals washed with pentane, and finally dried under vacuum for five minutes at room temperature to afford Fe(depe)$_2$(μ-N$_2$H)(B(C$_6$F$_5$)$_3$)(BAr$^F{}_4$) (**3**) as a crystalline solid (91.9 mg, 98%). For NMR analysis, in an identical preparation the cold C$_6$H$_5$F solution of **3** was transferred to a -30 °C NMR tube, and NMR spectra recorded at -45 °C without allowing the solution to warm beyond -30 °C. A sample of the solid was used to prepare a KBr pellet in a bolt-press for transmission IR analysis. ^{31}P-NMR showed a single product as composing 91% of phosphorus atoms in the sample, with the remaining 9% consisting of 4% *trans*-Fe(depe)$_2$(N$_2$)H and 5% of an unknown impurity. A single crystal was prepared by allowing pentane to diffuse into a solution of **4** in C$_6$H$_5$F at -30 °C. Samples of solid **3** are stable at room temperature under nitrogen for at least 4 hours. ^{31}P-NMR (C$_6$H$_5$F, -45 °C): 90.23 (1P, dd ($J_{31P\text{-}31P}$=44.7, 39.2), 78.56 (2P, h (37.3, 36.1), 72.01 (1P, dd ($J_{31P\text{-}31P}$ =47.0, 38.4). ^{19}F-NMR (C$_6$H$_5$F, -45 °C): -60.11 (BAr$^F{}_4$, 24F, s), -125.3 — -138.8 (6F, m (overlapping broad signals), -150.3 — -155.7 (3F, m (overlapping broad signals), -158.1 — -163.3 (6F, m (overlapping broad signals). ^{11}B-NMR (C$_6$H$_5$F, -45 °C): -1.09. ^{15}N-NMR (C$_6$H$_5$F, -45 °C): -49.31 (proximal –*N*, 1N, s (broad)), -140.71 (terminal –*N*, 1N, d ($J_{15N\text{-}1H}$=80.7). IR (KBr, cm^{-1}): ^{14}N-^{1}H: 3259, ^{15}N-^{1}H: 3247 (calc.: 3245); ^{14}N-^{11}B: 1421, ^{15}N-^{11}B: 1406 (calc.: 1401); ^{14}N-^{14}N: 1519, ^{15}N-^{15}N: 1465 (calc.: 1467), ^{14}N-^{56}Fe: 639, ^{15}N-^{56}Fe: 618 (calc.: 621).

Fe(depe)$_2$(μ-N$_2$H)(B(C$_6$F$_5$)$_3$)(BAr$^F{}_4$) (3-^{15}N):

A solution of **2-^{15}N** in C$_6$H$_5$F (60 μmol in 0.6 mL, 100 mM) was cooled to -30 °C in an NMR tube, under an argon atmosphere. A solution of H(OEt$_2$)$_2$BAr$^F{}_4$ (60 μmol in 0.2 mL C$_6$H$_5$F, 300 mM) cooled to -30 °C was rapidly added to **2** in one portion using a -30 °C syringe, and the chilled NMR tube rapidly inverted to mix the two components. NMR spectra were then recorded at -45 °C. To obtain a solid sample for KBr pellet IR spectroscopy, A solution of **2-^{15}N** in C$_6$H$_5$F (60 μmol in 0.6 mL, 100 mM) was cooled to -30 °C in scintillation vial, under an argon atmosphere. A solution of H(OEt$_2$)$_2$BAr$^F{}_4$ (60 μmol in 0.2 mL C$_6$H$_5$F, 300 mM) cooled to -30 °C was rapidly added to **2** in one portion using a -30 °C syringe, and the chilled vial shaken to mix the two components. The purple solution was then triturated with 6 mL -30 °C pentane, and allowed to

settle for 1 hour. The pentane was decanted and the purple solid dried under vacuum for 5 minutes at room temperature. The solid was then used to prepare a KBr pellet in a bolt-press and was analyzed by transmission IR spectroscopy.

Fig. ES9. ^{31}P NMR Spectrum with detail of P-P coupling:

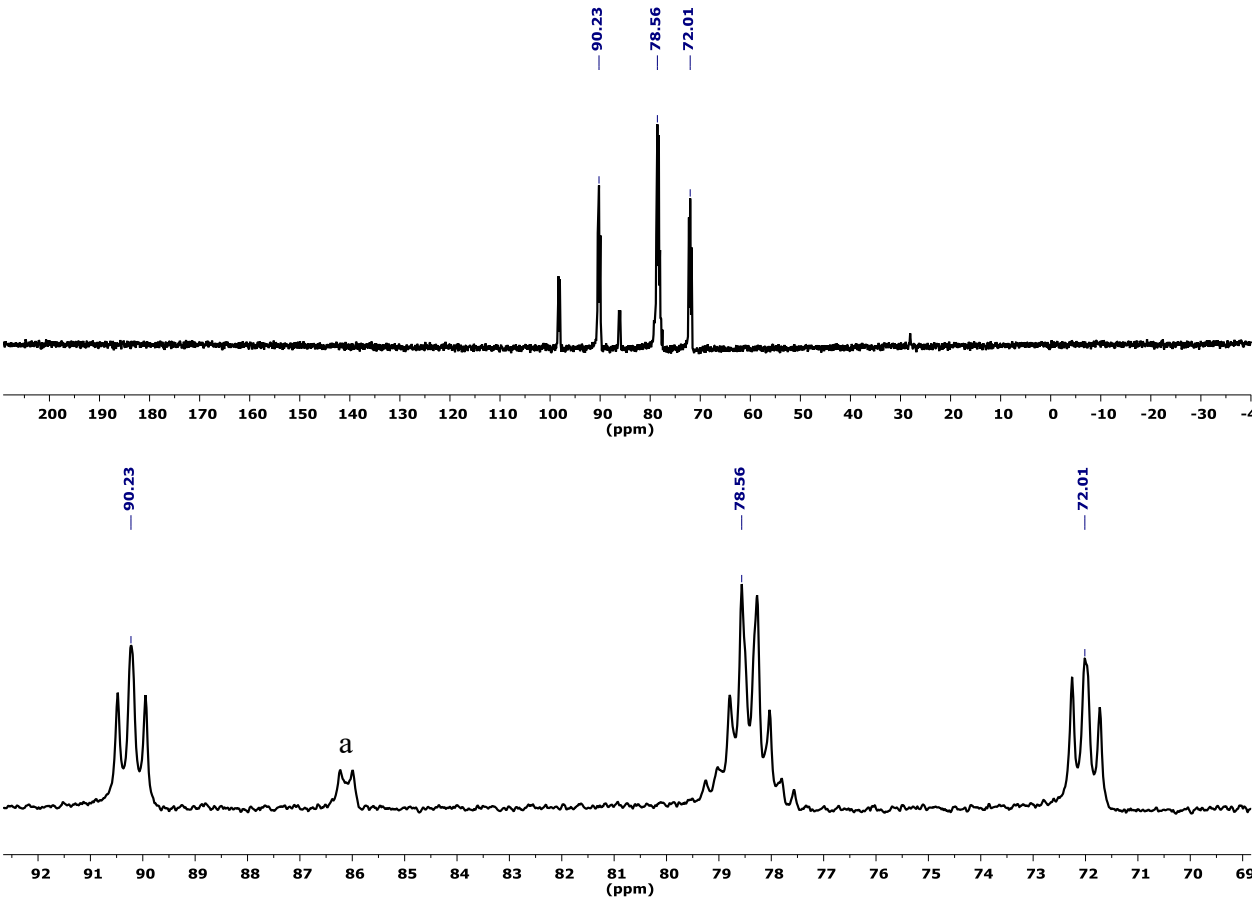

a: *trans*-Fe(depe)$_2$(N_2)H

Fig. ES10. ^{19}F NMR Spectrum with detail of complex $B(C_6F_5)_3$ region:

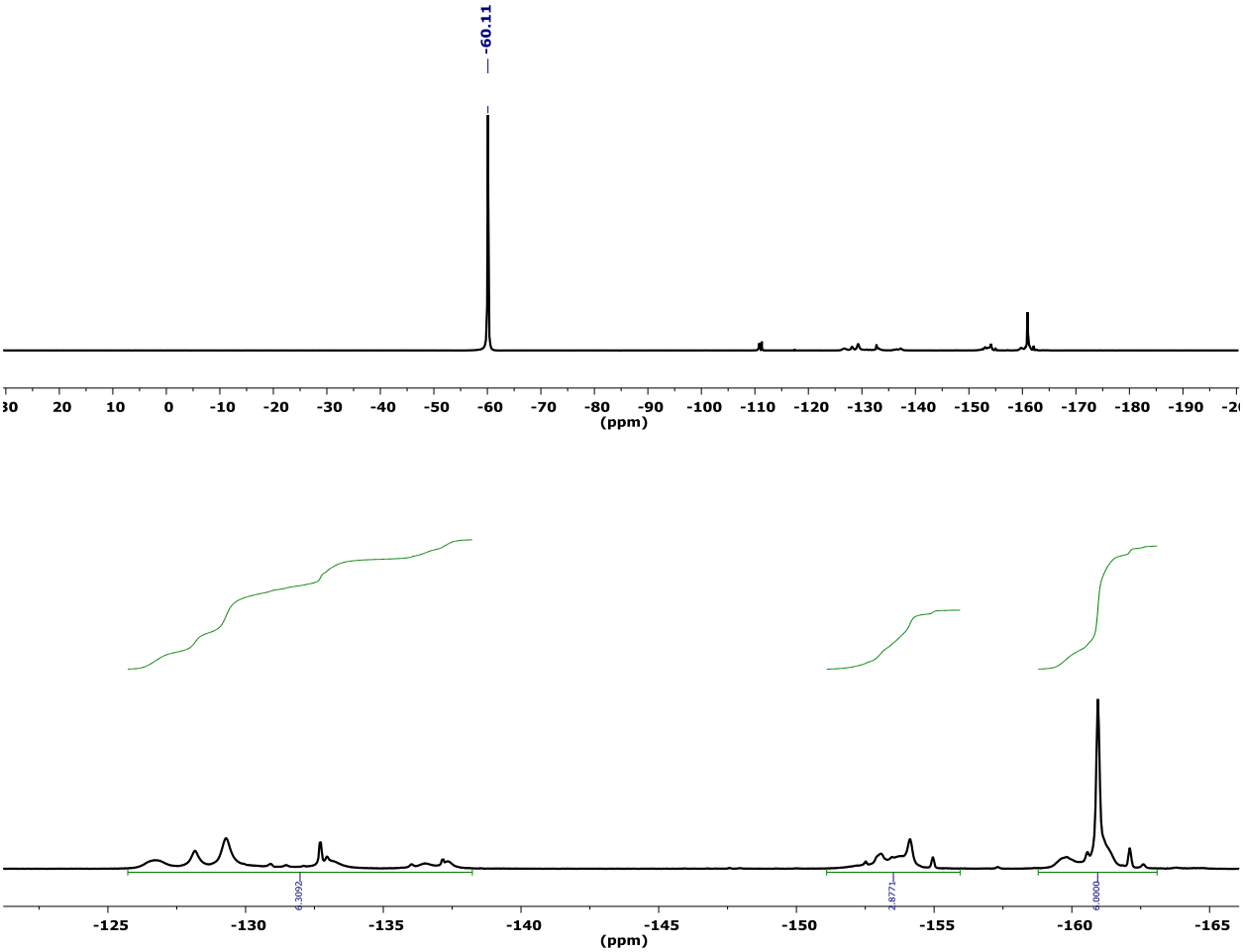

Fig. ES11. ^{11}B NMR Spectrum:

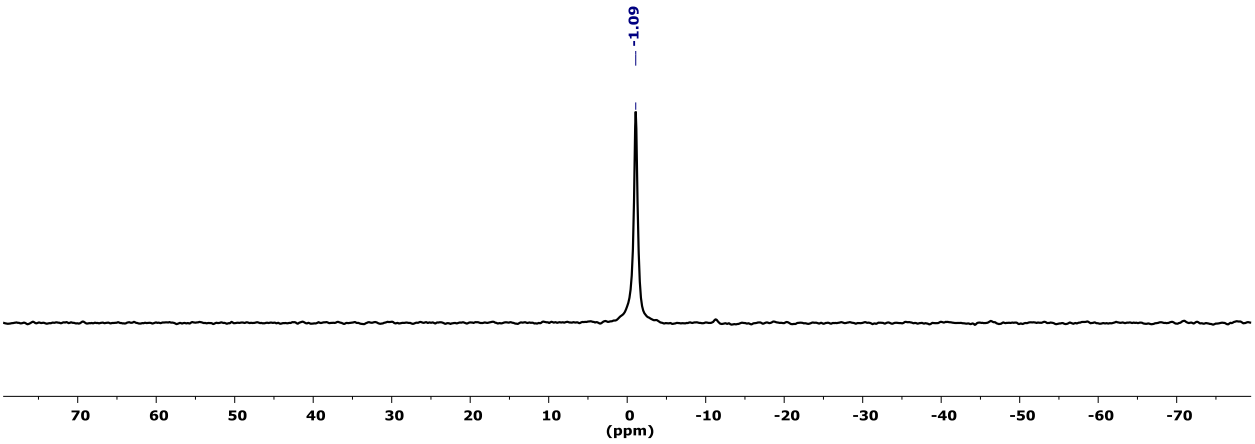

Fig. ES12. ^{15}N NMR Spectrum and ^{15}N-^{1}H decoupled NMR spectrum:

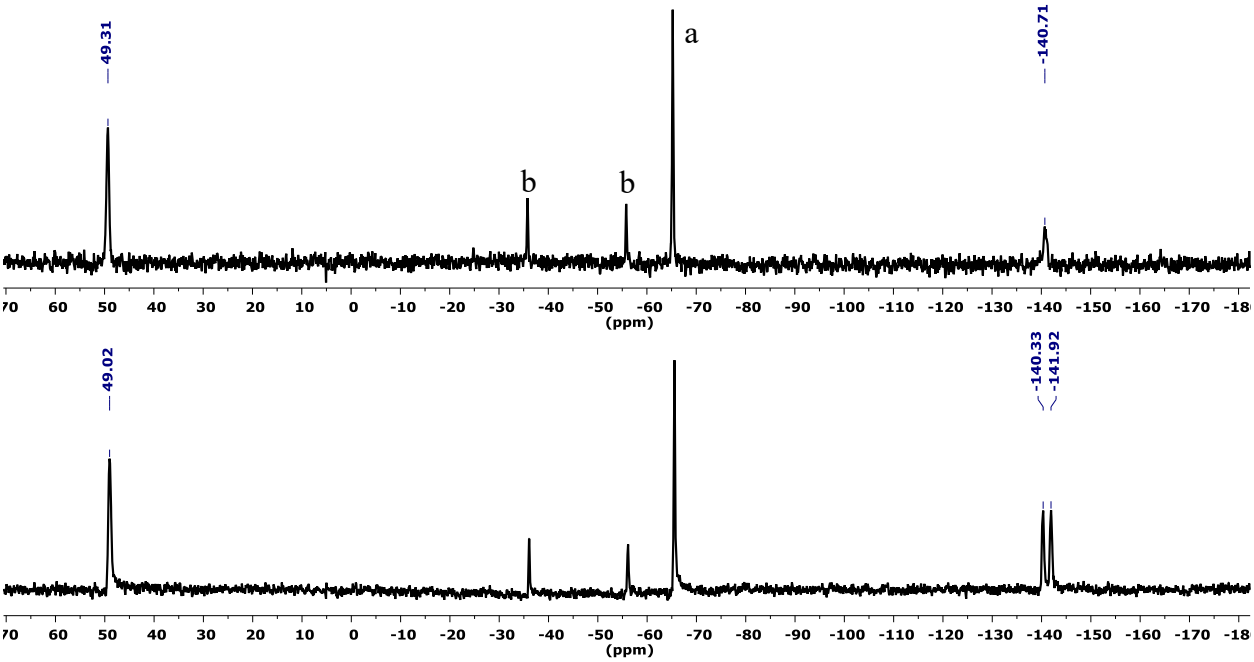

a: $^{15}N_2$; b: *trans*-Fe(depe)$_2$(N_2)H

Fig. ES13. IR spectrum

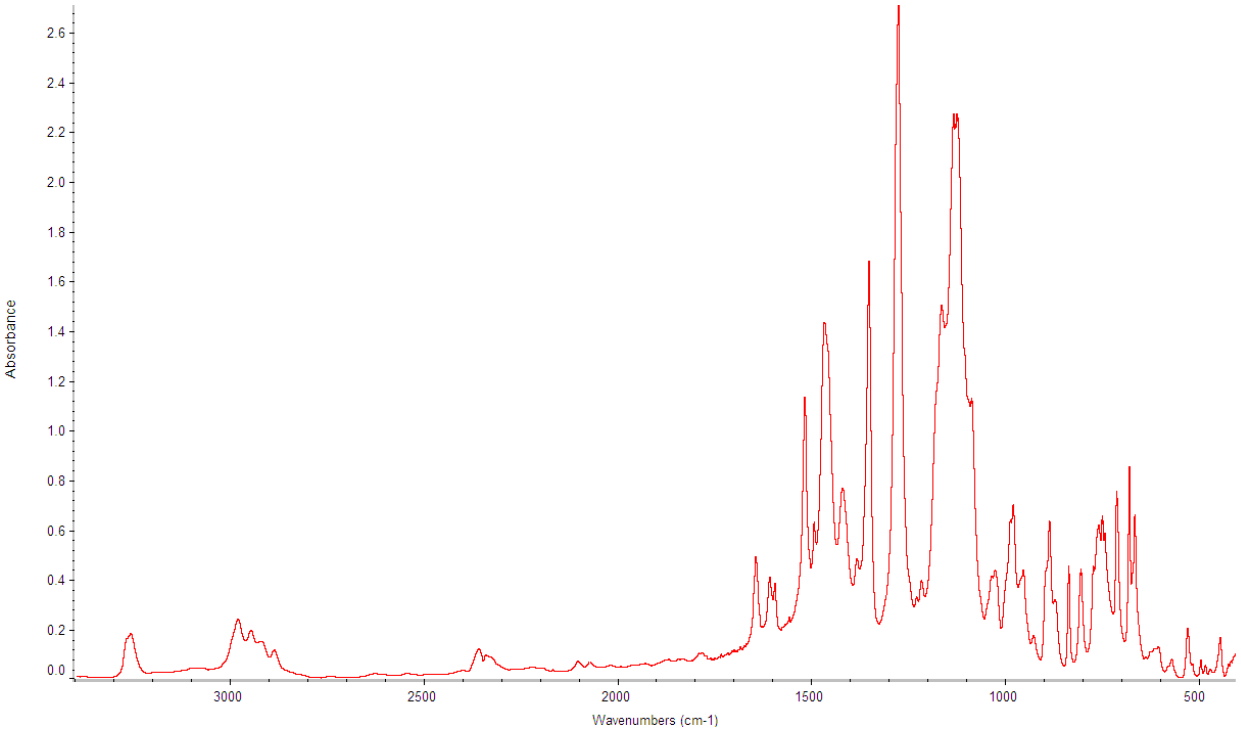

Fig. ES14. Highlighted N-H, N-N, N-B, and N-Fe stretches:

N-H Stretch (Blue: ^{14}N; Red: ^{15}N)

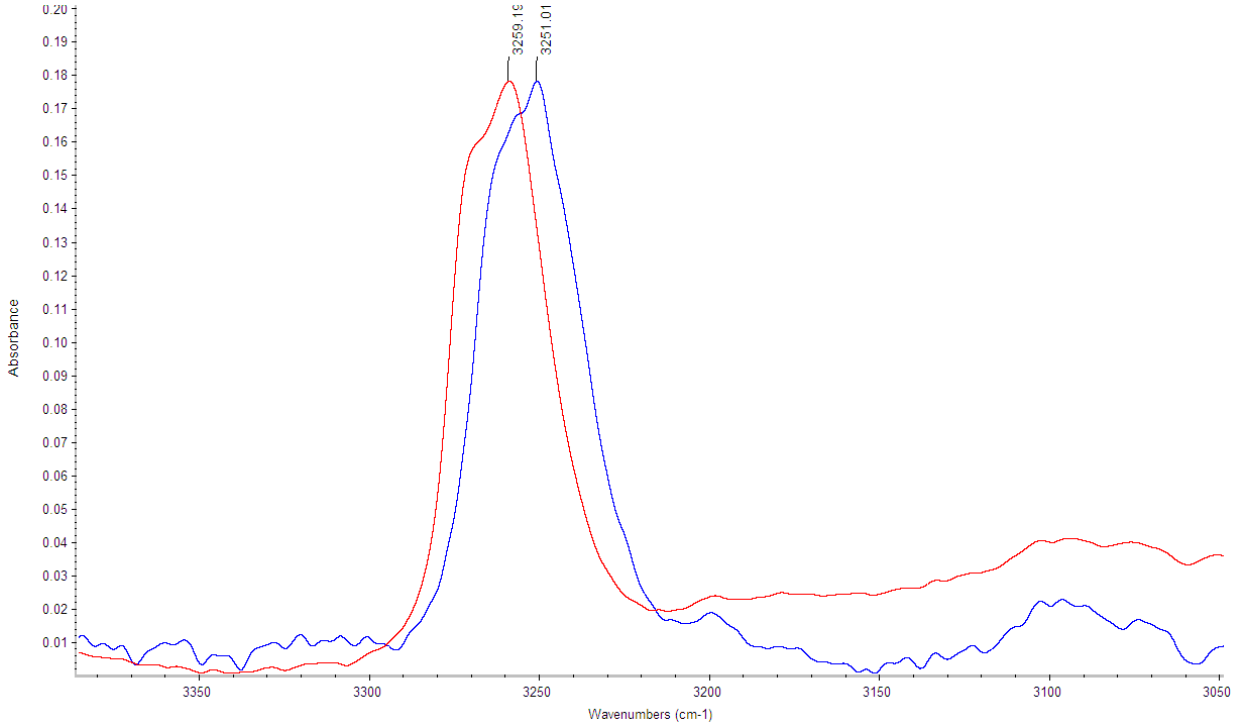

N-N Stretch (Blue: ^{14}N; Red: ^{15}N)

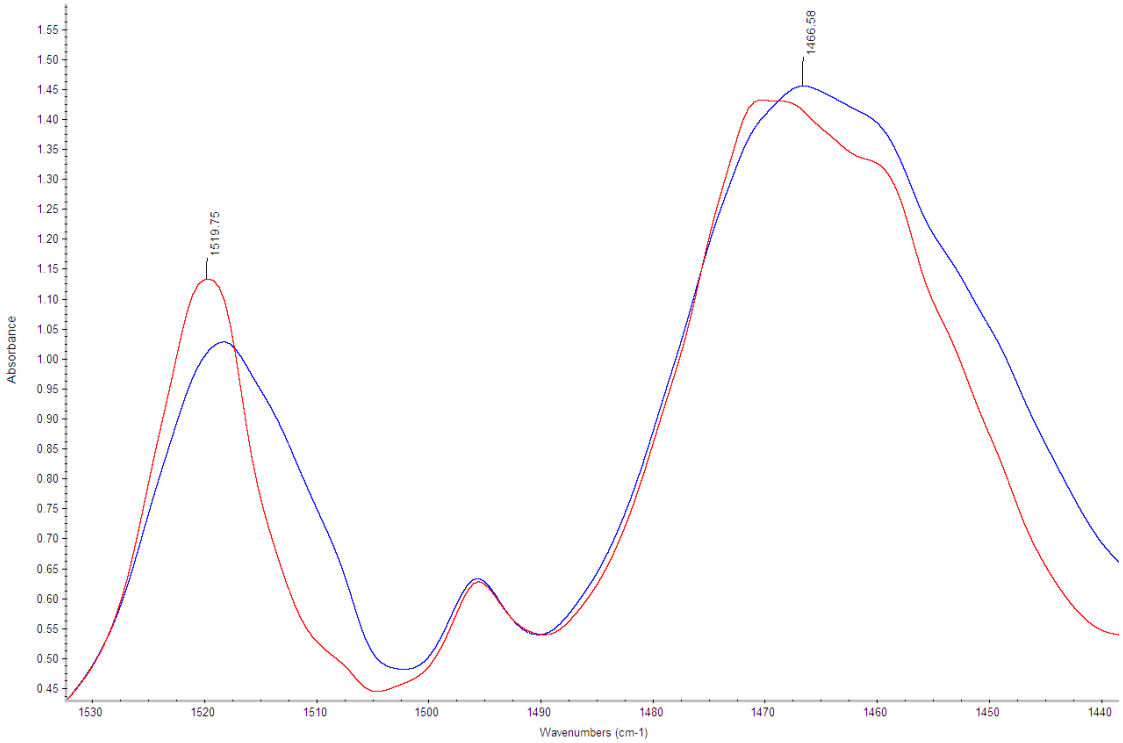

N-B Stretch (Blue: ^{14}N; Red: ^{15}N)

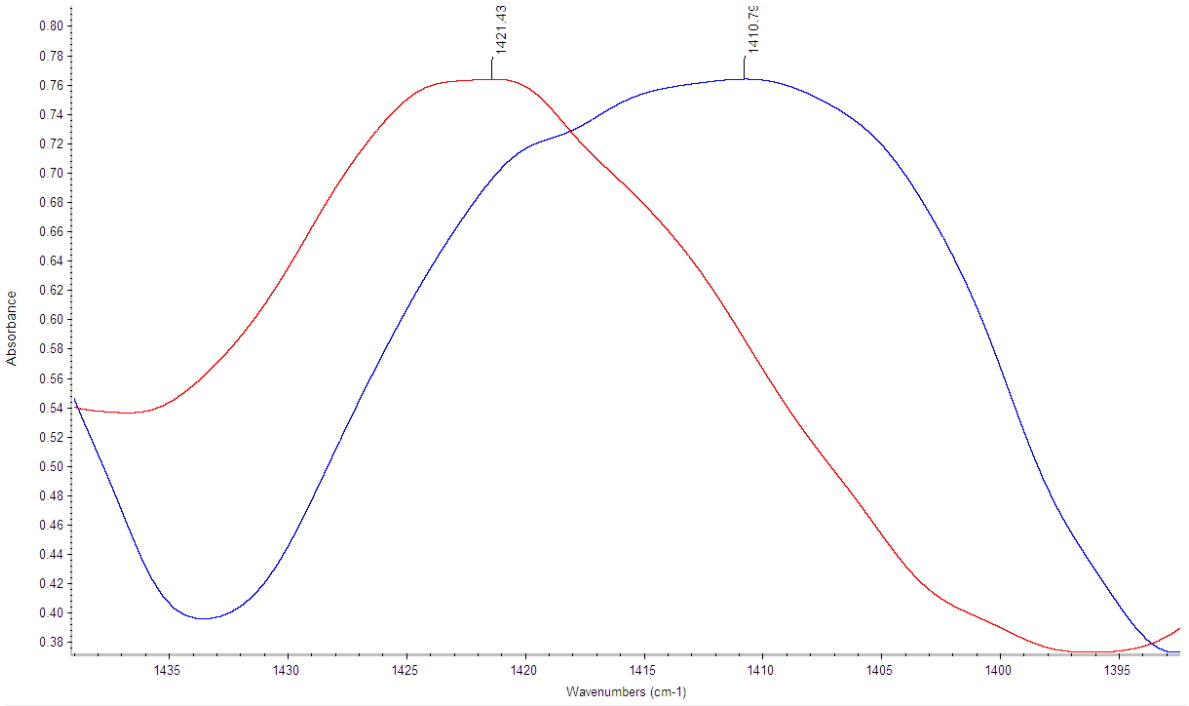

N-Fe Stretch (Blue: ^{14}N; Red: ^{15}N)

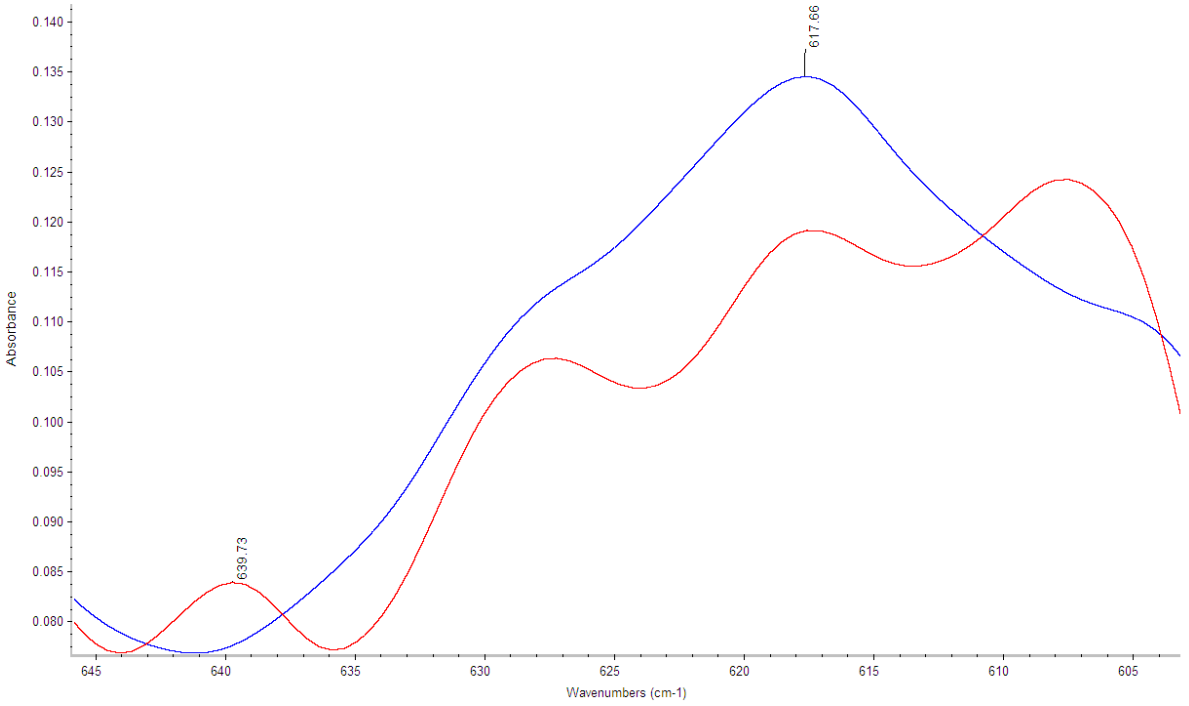

Fig. ES15. X-Ray Crystal Structure:

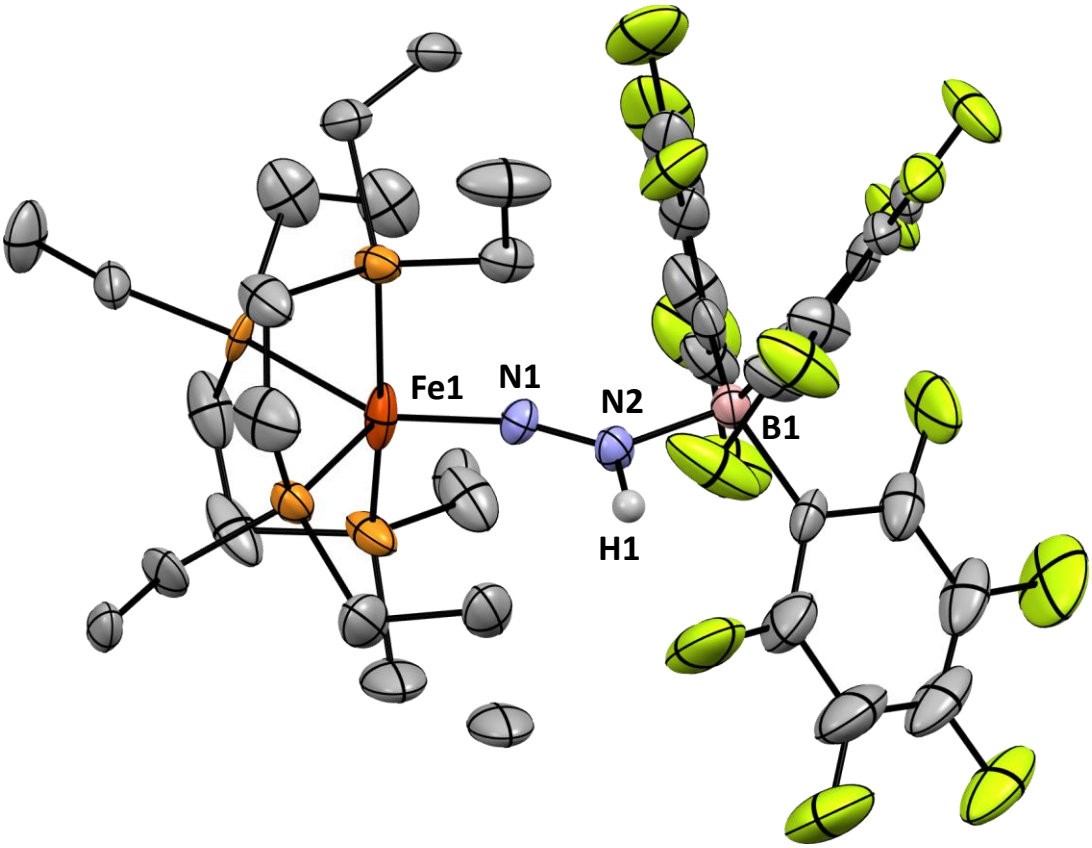

N1-N2: 1.25 Å; Fe1-N1: 1.67 Å; B1-N2-N1: 130 °

Fe(depe)$_2$(μ-N$_2$)Fe(^{i}Pr$_2$Tp)(BAr$^F_4$) (4):

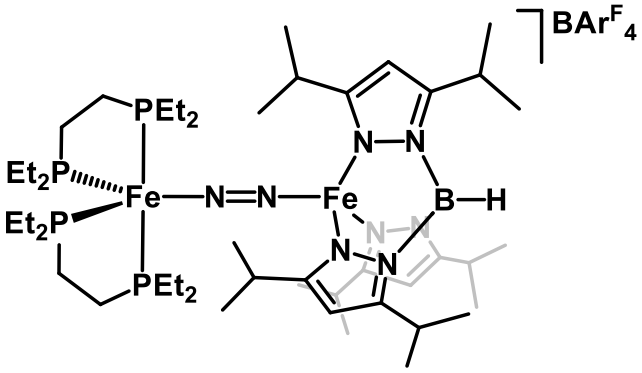

Fe(depe)$_2$N$_2$ (1) (20.0 mg, 40.0 μmol), Fe(II)(^{i}Pr$_2$Tp)Cl (22.2 mg, 40.0 μmol), and NaBAr$^F_4$ (35.4 mg, 40.0 mg) were combined in a scintillation vial. C_6H_5F (2 mL) was then added at room temperature and the mixture stirred for three minutes, generating a dark brown solution and a colorless precipitate. The mixture was filtered and the filtrate evaporate under vacuum to afford Fe(depe)$_2$(μ-N$_2$)Fe(^{i}Pr$_2$Tp)(BAr$^F_4$) (4) as a dark brown/green powder (69.0 mg, 91% yield). A

single crystal suitable for X-ray diffraction was prepared by layering pentane over a C6H5F solution of **4**. A solution of **4** in C_6H_5F was used for transmission IR spectroscopy. ^{11}B-NMR (C_6D_6): -6.01; ^{31}P-NMR (C_6D_6): 80.34, 80.11. µeff (Evans Method): 4.77 (3.87 unpaired electrons; S=2). UV/Vis (C_6H_6): 441 (ε=2780), 902 (IVCT, ε=1680). Solvent-Dependent IVCT band peak position, absorption coefficient (ε), full width at half max (FWHM): C_6H_6: 910 nm, ε=1700 $M^{-1}cm^{-1}$, FWHM=3398 cm^{-1}; C_6H_5F: 914 nm, ε=993 $M^{-1}cm^{-1}$, FWHM=3276 cm^{-1}; tetrahydrofuran: 905 nm, ε=857 $M^{-1}cm^{-1}$, FWHM=2872 cm^{-1}. IR (C6H5F, cm^{-1}): 1824.

Fig. ES16. ^{11}B NMR spectrum:

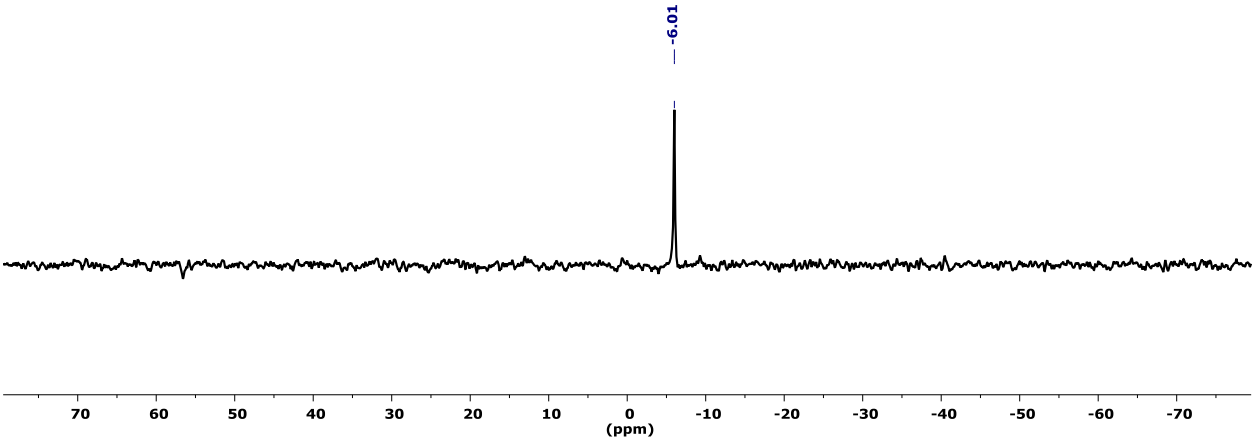

Fig. ES17. ^{31}P NMR spectrum:

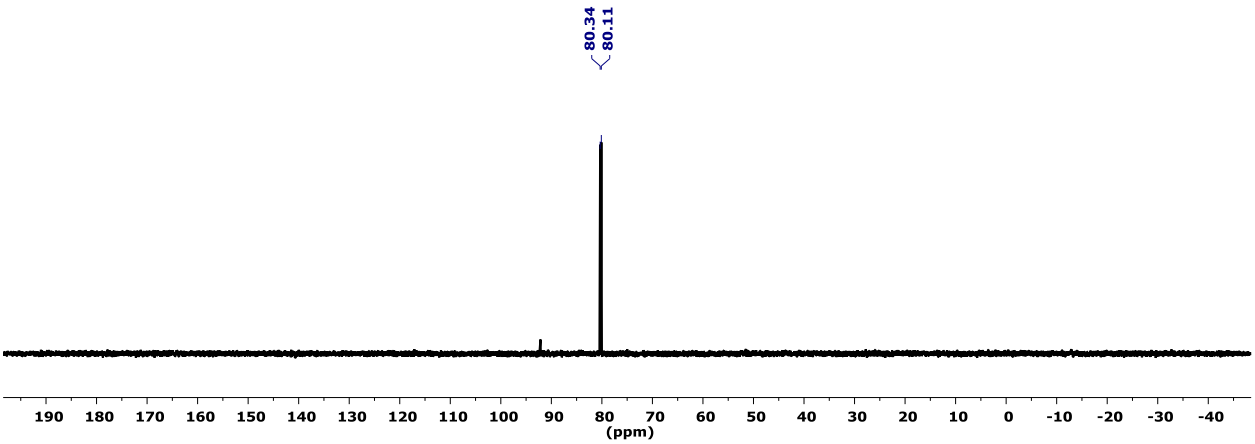

Fig. ES18. UV/Vis spectrum:

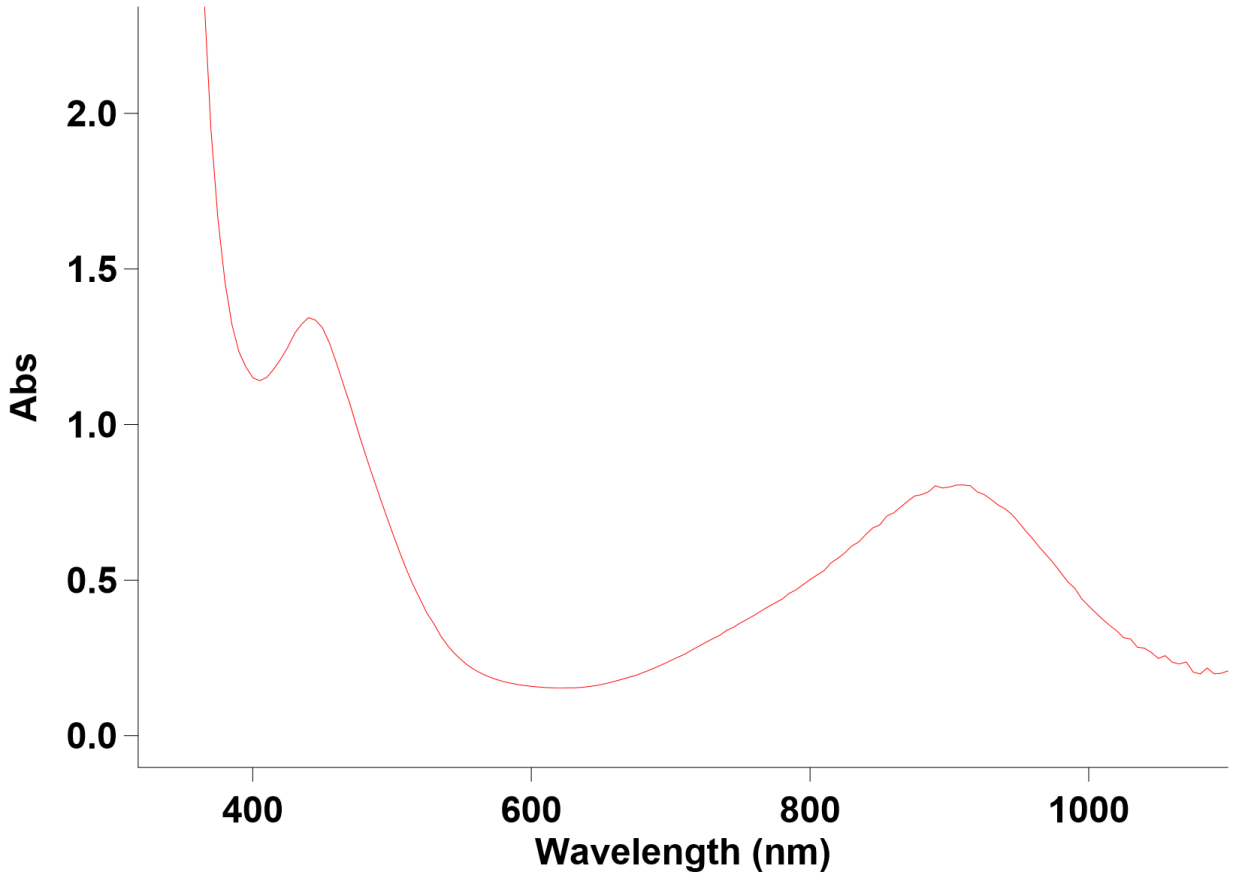

Fig. ES19. IR spectrum:

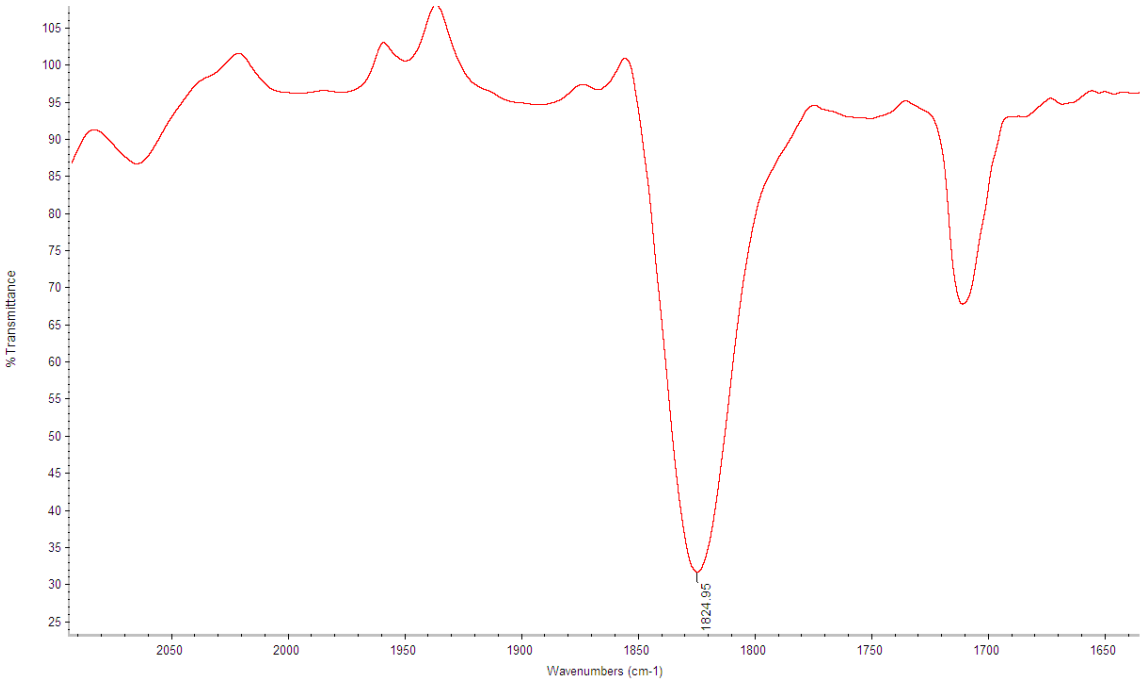

Fig. ES20. X-Ray Crystal Structure:

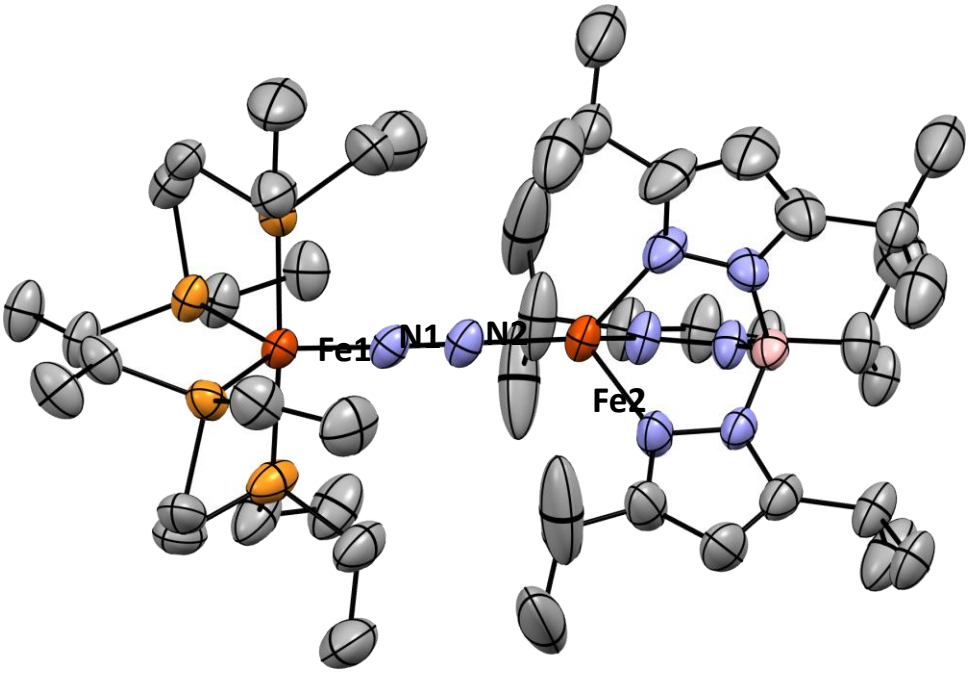

Fe1-N1: 1.742 Å; N1-N2: 1.177 Å; N2-Fe2: 1.884 Å; Fe1-N1-N2: 175.14°; Fe2-N2-N1: 173.38°

Other assym. unit:

Fe1-N1: 1.744 Å; N1-N2: 1.181 Å; N2-Fe2: 1.887 Å; Fe1-N1-N2: 177.67°; Fe2-N2-N1: 176.46°

In-Situ Generation of Fe-N_2-LA Adducts

General Procedure:

$Fe(depe)_2(N_2)$ (10 µmol, 4.9 mg) and 10 µmol of a Lewis acid were combined in a small 2 mL vial equipped with a teflon lined septum (a gas chromatography sample vial). To this was added 0.5 mL solvent (Et_2O if LA=$M^+BAr^F{}_4^-$ (M= Na, K, Rb, Cs) or $LiB(C_6F_5)_4$; C_6H_5F if LA=BR_3 (R=2,6-F_2-Ph, 2,4,6-F_3-Ph, C_6F_5, OC_6F_5, or F)), and the vial shaken vigorously for 30 seconds to afford a homogeneous solution. The solution was then transferred via syringe into a transmission IR solution cell and IR spectra were immediately recorded.

Fig. ES21. IR Spectra for All Reported Adducts:

$Fe(depe)_2(\mu\text{-}N_2)(Li)\ B(C_6F_5)_4$

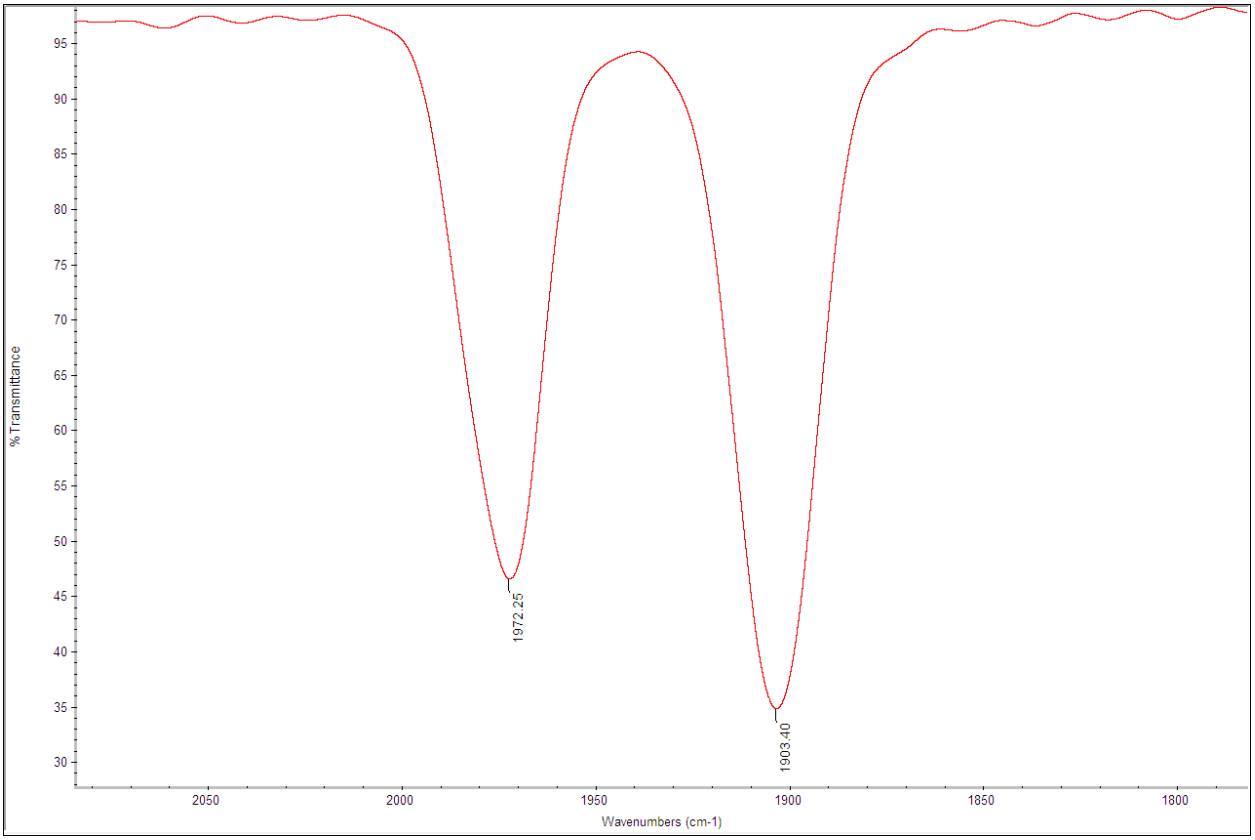

$Fe(depe)_2(\mu\text{-}N_2)(Na)\ BAr^F{}_4$

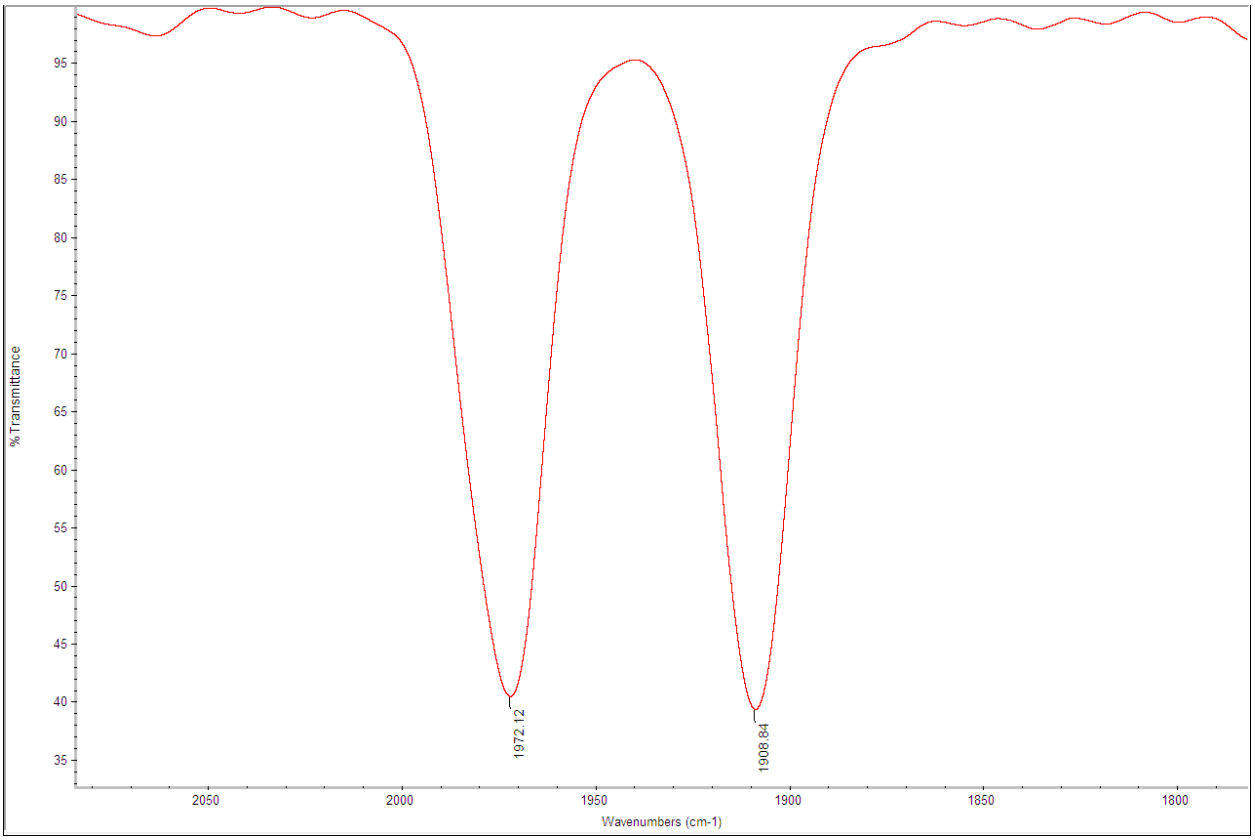

$Fe(depe)_2(\mu\text{-}N_2)(K)\ BAr^F{}_4$

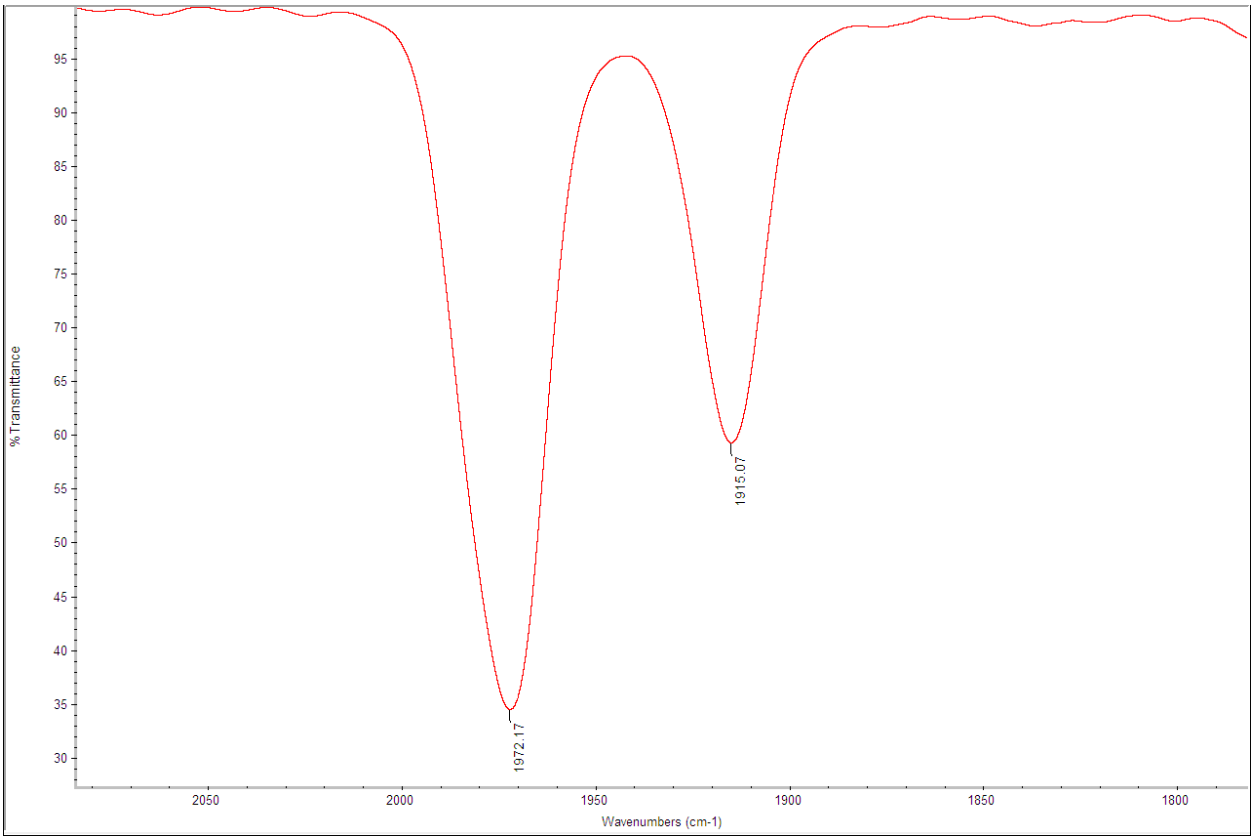

$Fe(depe)_2(\mu\text{-}N_2)(Rb)\ BAr^F{}_4$

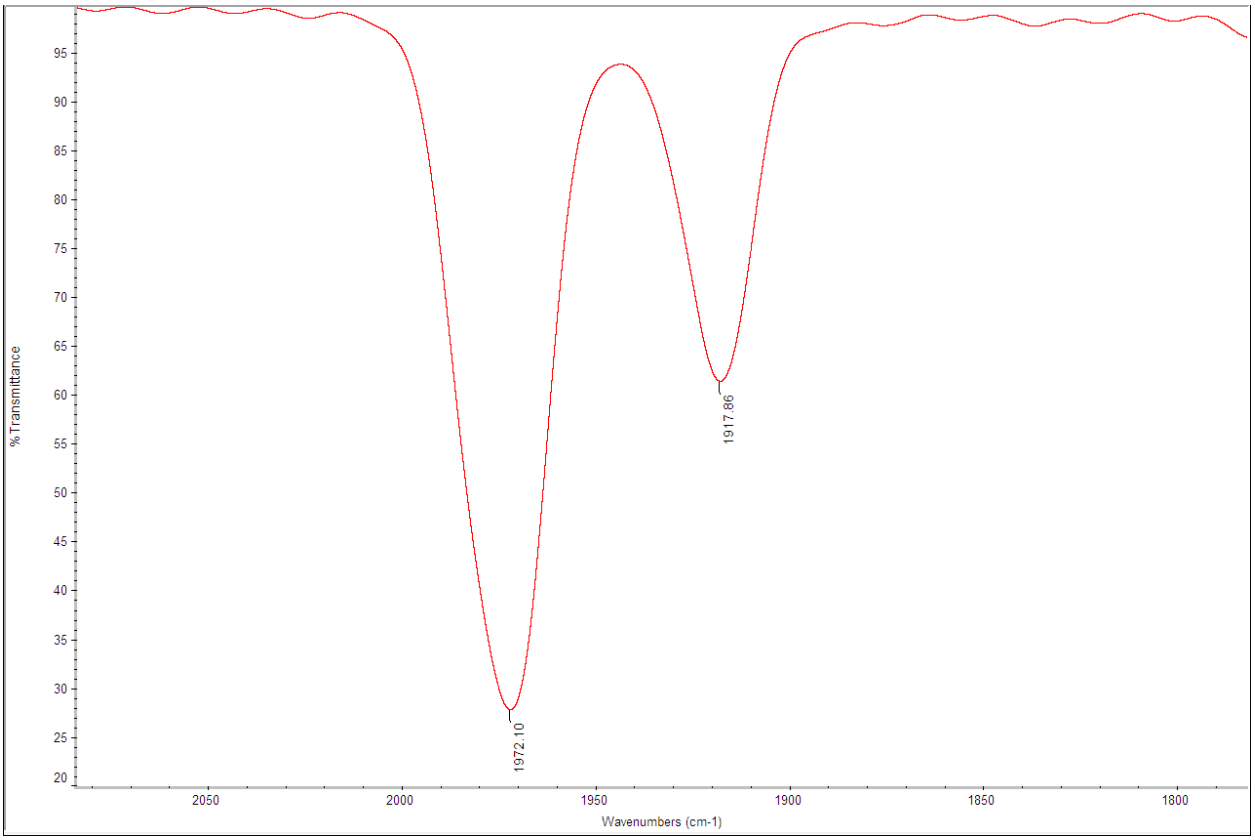

$Fe(depe)_2(\mu\text{-}N_2)(Cs)\ BAr^F{}_4$

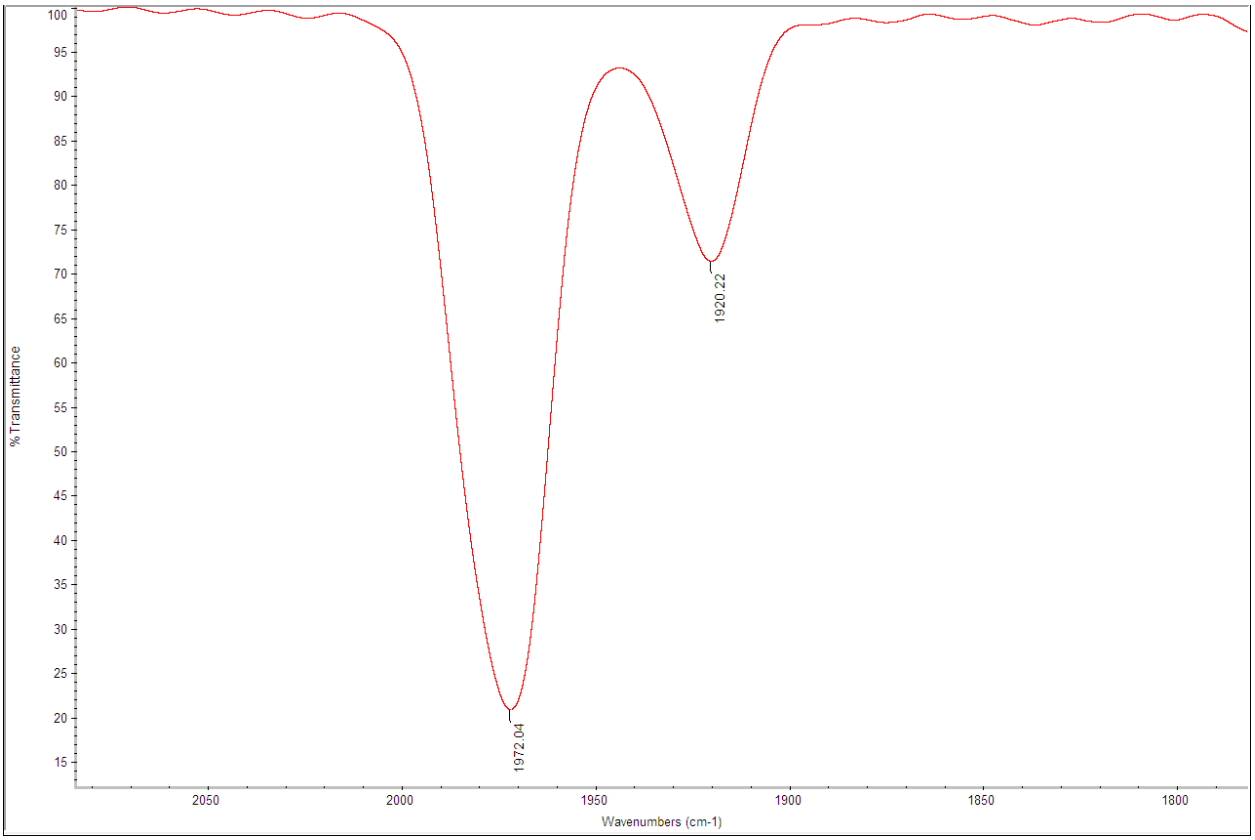

$Fe(depe)_2(\mu\text{-}N_2)(B(2,6\text{-}F_2\text{-}Ph)_3)$

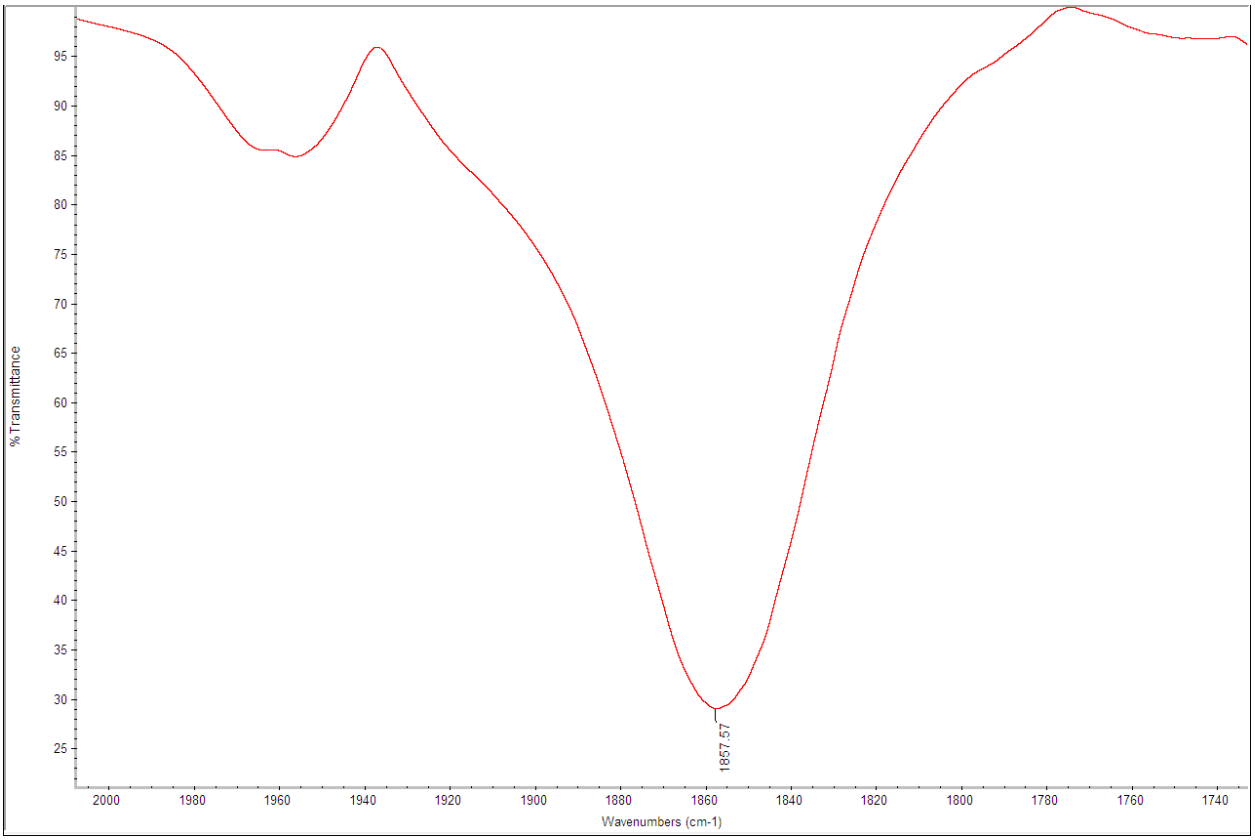

$Fe(depe)_2(\mu\text{-}N_2)(B(2,4,6\text{-}F_3\text{-}Ph)_3)$

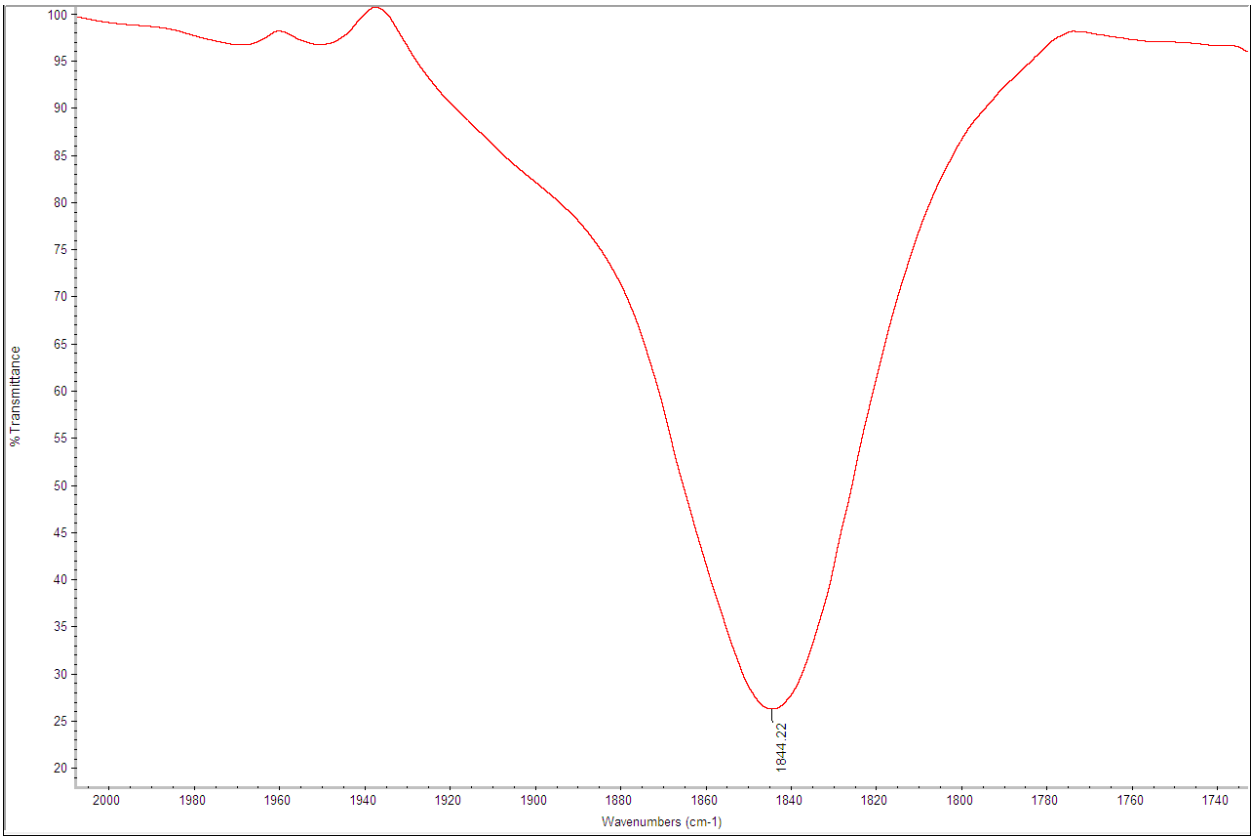

$Fe(depe)_2(\mu\text{-}N_2)(B(C_6F_5)_3)$

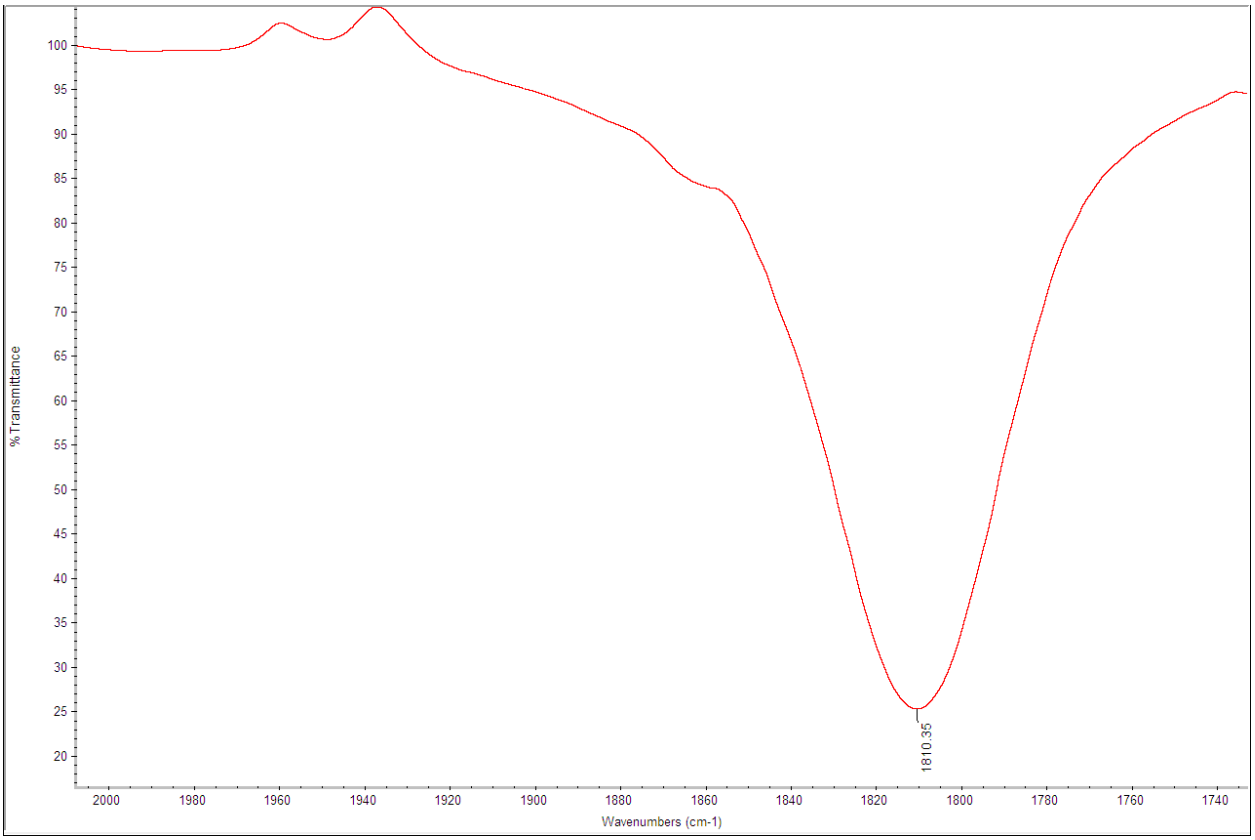

$Fe(depe)_2(\mu\text{-}N_2)(B(OC_6F_5)_3)$

$Fe(depe)_2(\mu\text{-}N_2)(BF_3)$

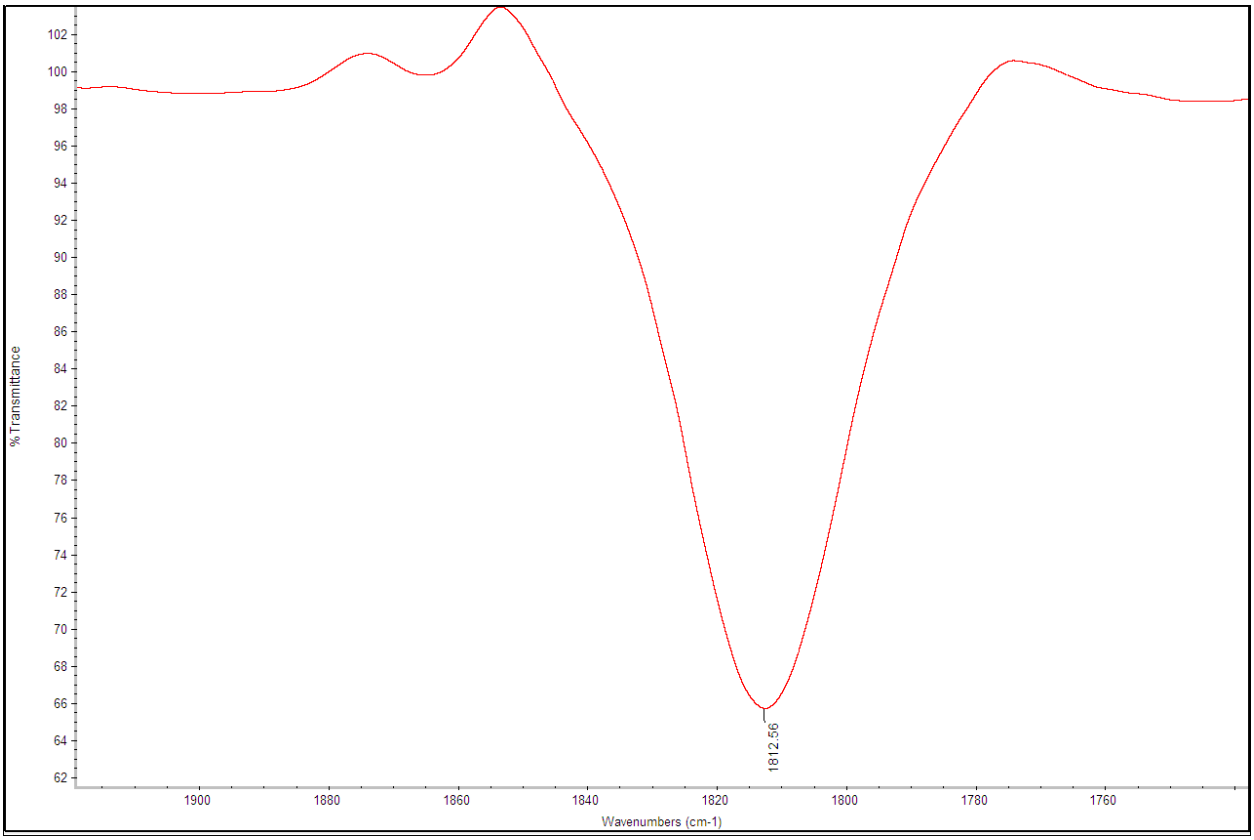

Determination of Equillibrium Constants of Fe-N_2-LA Adducts

General Procedure for LA=BR_3 in C_6H_5F (R=2,6-F_2-Ph, 2,4,6-F_3-Ph, C_6F_5, or OC_6F_5):

A C_6H_5F solution containing $Fe(depe)_2(N_2)$ (0.100 M) and diisopropyl ketone (0.100 M) (50.0 µL, 5.00 µmol) was added to a solution of Lewis acid (0.050M, 100 µL, 5.00 µmol) in a 2 mL vial equipped with a teflon lined septum (a gas chromatography sample vial) using a volumetric syringe. The vial was shaken vigorously for 30 seconds to afford a homogeneous solution. The solution was then transferred via syringe into a transmission IR solution cell and IR spectra were immediately recorded. Concentrations were evaluated based on the relative integration of $Fe(depe)_2(N_2)$ vs. the diisopropyl ketone internal standard, as compared to an IR spectrum taken of a 0.02 M stock of a 1:1 mixture of $Fe(depe)_2(N_2)$ and diisopropyl ketone (relative integrated IR absorption: 6.55).

General Procedure for LA=M^+ in Et_2O (M^+=[Li $B(C_6F_5)_4$, Na BAr^F_4, K BAr^F_4, Rb BAr^F_4, Cs BAr^F_4]):

A Et_2O solution containing $Fe(depe)_2(N_2)$ (40.0 mM) and diisopropyl ketone (40.0 mM) (250 µL, 10.0 µmol) was added to a solution of Lewis acid (40.0 mM, 250 µL, 10.0 µmol) in a 2 mL vial equipped with a teflon lined septum (a gas chromatography sample vial) using a volumetric

syringe. The vial was shaken vigorously for 30 seconds to afford a homogeneous solution. The solution was then transferred via syringe into a transmission IR solution cell and IR spectra were immediately recorded. Concentrations were evaluated based on the relative integration of $Fe(depe)_2(N_2)$ vs. the diisopropyl ketone internal standard, as compared to an IR spectrum taken of a 0.02 M stock of a 1:1 mixture of $Fe(depe)_2(N_2)$ and diisopropyl ketone (relative integrated IR absorption: 8.56).

Fig. ES22. Tabulated IR integrals and Binding Constants for Lewis Acids Li $B(C_6F_5)_4$, Na BAr^F_4, K BAr^F_4, Rb BAr^F_4, Cs BAr^F_4 in Et_2O.

LA (trial)	Integrals:			$Fe(depe)_2(N_2)$ Concentration	K (M^{-1}):
	$Fe(depe)_2(N_2)$	$Fe(depe)_2(N_2)$-LA	iPr_2CO		
Li (1)	5.779	8.393	2.484	0.00710	4.3(8)E+2
Li (2)	6.988	9.917	2.511	0.00849	
Na (1)	8.369	7.945	2.983	0.00856	3.6(2)E+2
Na (1)	8.012	8.906	2.928	0.00835	
Na (1)	7.468	8.17	2.806	0.00812	
K (1)	9.822	4.105	2.55	0.01176	1.4(1)E+2
K (1)	11.332	4.278	2.755	0.01255	
K (1)	10.472	4.381	2.659	0.01202	
Rb (1)	11.732	3.66	2.734	0.01310	1.2(4)E+2
Rb (1)	10.925	3.415	2.596	0.01284	
Rb (1)	10.66	3.758	2.569	0.01266	
Cs (1)	14.259	2.266	2.962	0.01469	9.4(5)E+1
Cs (1)	12.615	2.483	2.749	0.01401	
Cs (1)	12.877	2.418	2.804	0.01402	

Fig. ES23. Tabulated IR integrals and Binding Constants for Lewis Acids LA= BR_3 (R=2,6-F_2-Ph, 2,4,6-F_3-Ph, C_6F_5, or OC_6F_5) in C_6H_5F.

LA (trial)	Integrals:			$Fe(depe)_2(N_2)$ Concentration	K (M^{-1}):
	$Fe(depe)_2(N_2)$	$Fe(depe)_2(N_2)$-LA	iPr_2CO		
$B(2,6\text{-}F_2\text{-}Ph)_3$ (1)	1.531	27.627	2.593	0.002299	4.6(9)E+3
$B(2,6\text{-}F_2\text{-}Ph)_3$ (2)	1.83	28.306	2.519	0.002828	
$B(2,6\text{-}F_2\text{-}Ph)_3$ (3)	1.782	27.93	2.574	0.002695	
$B(2,4,6\text{-}F_3\text{-}Ph)_3$ (1)	0.564	29.625	2.367	0.000928	3.6(8)E+4
$B(2,4,6\text{-}F_3\text{-}Ph)_3$ (2)	0.58	26.568	2.021	0.001117	
$B(2,4,6\text{-}F_3\text{-}Ph)_3$ (3)	0.525	29.85	2.434	0.00084	
$B(C_6F_5)$ (1)	0.374	29.395	2.327	0.000626	7.9(8)E+4
$B(C_6F_5)$ (2)	0.499	30.355	2.344	0.000829	
$B(C_6F_5)$ (3)	0.358	29.495	2.532	0.00055	
$B(OC_6F_5)_3$ (1)	5.576	5.942	2.098	0.010348	2.1(7)E+2
$B(OC_6F_5)_3$ (2)	5.525	6.48	2.049	0.010498	
$B(OC_6F_5)_3$ (3)	5.316	5.644	2.04	0.010146	

Fig. ES24. Sample IR spectra of binding constant experiments for LA= Li $B(C_6F_5)_4$, Na BAr^F_4, K BAr^F_4, Rb BAr^F_4, Cs BAr^F_4 in Et_2O.

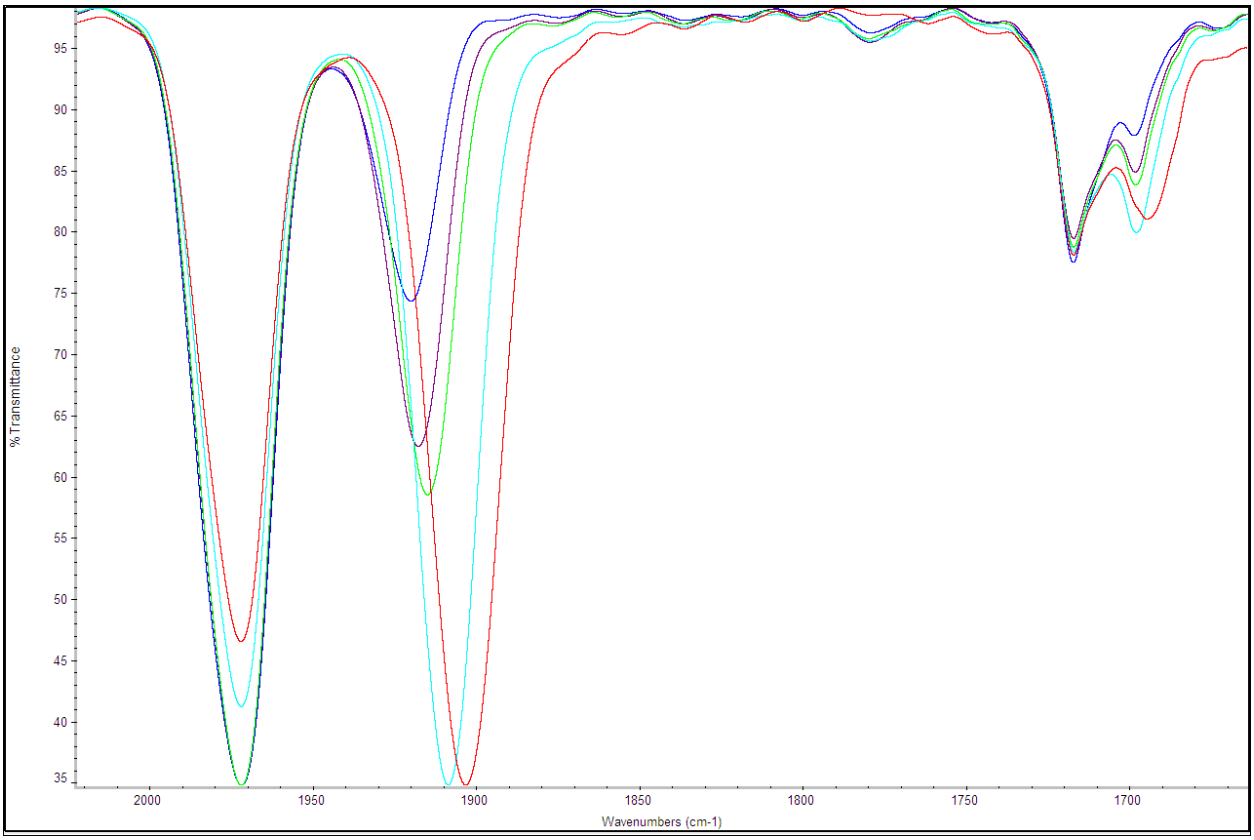

Blue: Cs^+; Purple: Na^+; Green: K^+; Cyan: Na^+; Red: Li^+

Fig. ES25. Sample IR spectra of binding constant experiments for LA= BR_3 (R=2,6-F_2-Ph, 2,4,6-F_3-Ph, C_6F_5, or OC_6F_5) in C_6H_5F.

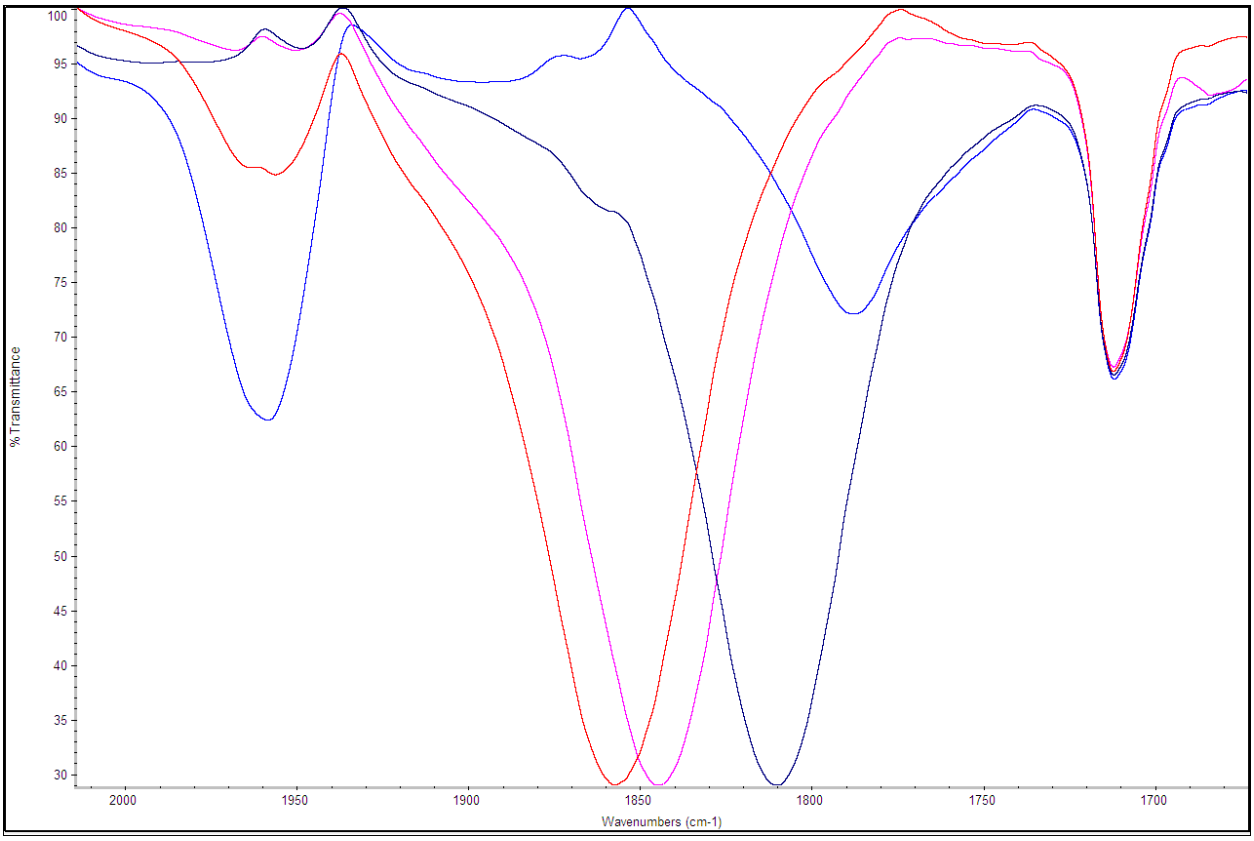

Red: B(2,6-F_2-Ph)$_3$; Purple: B(2,4,6-F_2-Ph)$_3$; Navy: B(C_6F_5)$_3$; Blue: B(OC_6F_5)$_3$

Acceptor Number Determination for Lewis Acids

An aliquot (0.5 mL) of triethylphosphine oxide solutions (75 mM) in either fluorobenzene or diethyl ether were added to the Lewis Acid (0.037 mmol). The $^{31}P\{^1H\}$ NMR were collected at 25 °C and externally referenced to 85% H_3PO_4. The measured resonances converted to Acceptor Number as described by the equation:

$$AN = 2.21 \times (\delta_{sample} - 41.0)$$

Fig. ES26. Tabulated $^{31}P\{^{1}H\}$ NMR shifts and Acceptor Number (AN) of Lewis acids in the presence of 1 equivalent of triethylphosphine oxide in specified solvent.

LA	Solvent	δ $^{31}P\{^{1}H\}$ Shift	AN
[Na][BAr^F_4]	PhF	57.00	35.36
[Li][$B(C_6F_5)_4$]	PhF	59.25	40.32
$B(C_6H_5)_3$	PhF	68.15	60.01
B(4-F-Ph)$_3$	PhF	69.28	62.51
B(2,6-F_2-Ph)$_3$	PhF	71.51	76.25
B(2,4,6-F_3-Ph)$_3$	PhF	72.26	69.07
$B(C_6F_5)_3$	PhF	76.91	79.37
BF_3 (Et_2O)	PhF	77.82	81.37
$B(OC_6F_5)_3$	PhF	80.95	89.46
None	PhF	47.20	13.7
[Cs][BAr^F_4]	Et_2O	52.98	26.48
[Rb][BAr^F_4]	Et_2O	53.50	27.63
[K][BAr^F_4]	Et_2O	54.19	29.15
[Na][BAr^F_4]	Et_2O	56.48	34.20
[Li][$B(C_6F_5)_4$]	Et_2O	58.13	37.85
None	Et_2O	48.43	16.42

Electrochemical Analysis

CV and DPV were measured in fluorobenzene with 0.1 M [NBu_4][BAr^F_4] as the electrolyte with platinum working, platinum counter, and a silver wire pseudo-reference electrodes. The electrolyte solution was cooled to -40 °C in an acetonitrile dry ice bath, prior to adding the measured compound. Lewis acid adducts of **1** were prepared in fluorobenzene in situ via addition of a stock solution of each Lewis acid to an aliquot of a stock solution of **1** to yield a 30 mM stock solution of the adduct. The resulting adduct stock solutions were cooled in the dry ice acetonitrile bath prior to addition of aliquots of analyte to the electrolyte to a concentration of 8 mM **1-LA**. The measured DPV and CV were referenced to decamethylferrocene (Fc*). An independent measurement of the difference in redox potential between Fc and Fc* was then used to reference vs Fc.

Fig. ES27. Cyclic Voltammogram of Fc and Fc* in 0.1 M [NBu_4][BAr^F_4] fluorobenzene at 25 °C (black) and -45 °C (red).

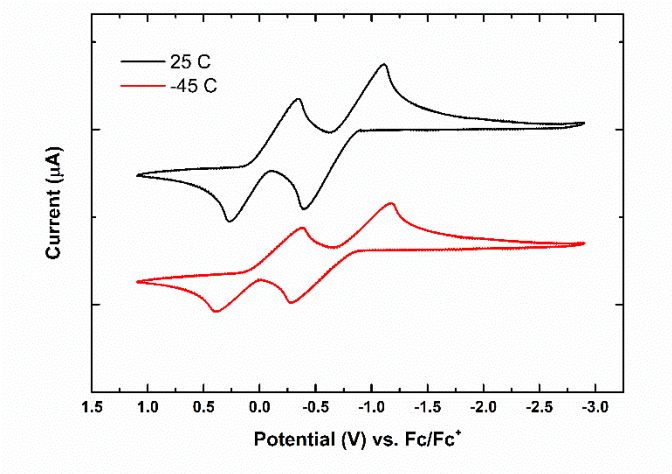

Fig. ES28. Cyclic Voltammogram of 1 and Lewis acid adducts in 0.1 M [NBu_4][$BAr^F{}_4$] fluorobenzene cooled in a dry ice acetonitrile bath. For the voltammogram of the $B(OC_6F_5)_3$ adduct, 10 equivalents of the Lewis acid were added.

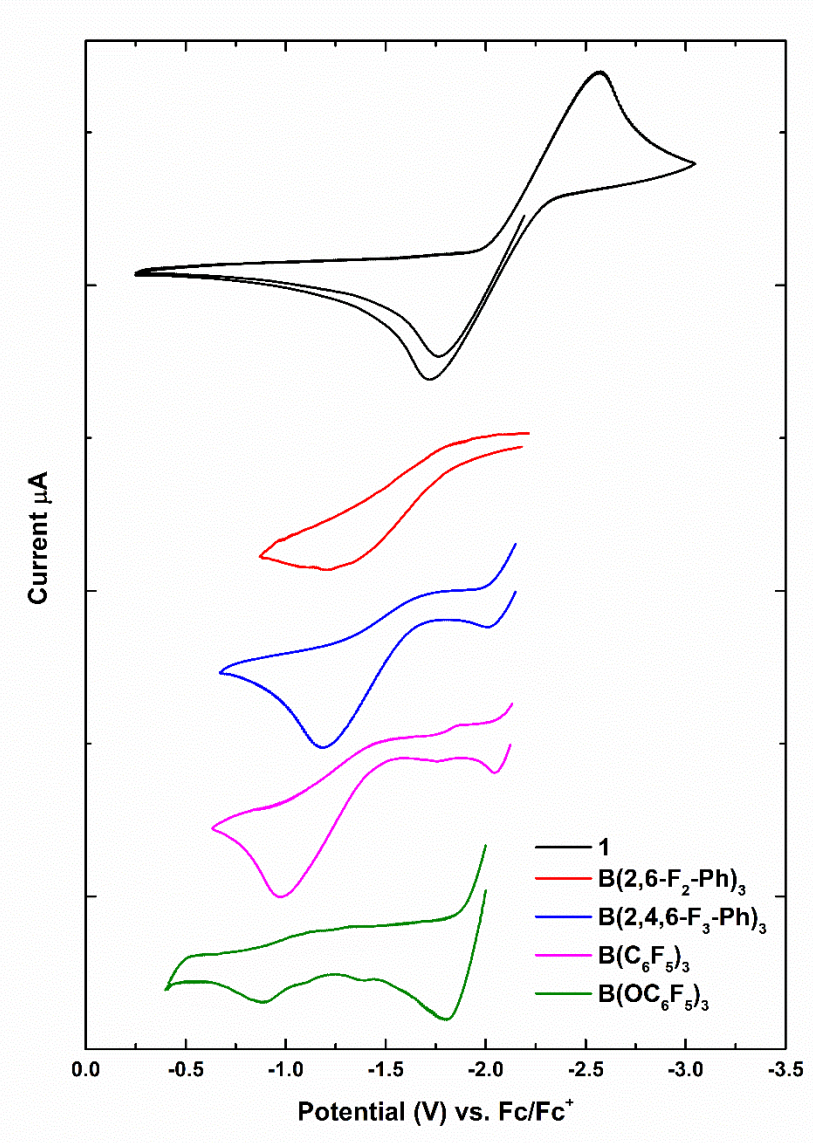

Irreversible oxidation of **2** is likely due to the high instability of $\mathbf{2}^+$. This was validated through the lack of reactivity between $Fe(I)(depe)_2(N_2)^+$ and six equivalents of $B(C_6F_5)_3$ at room temperature or excess BF_3 gas at -45 °C in fluorobenzene, as assessed both through monitoring the continued presence of $Fe(I)(depe)_2(N_2)^+$ via its N-N stretch at 2065 cm^{-1} and the appearence of no new peaks in the region between 2200 and 1700 cm^{-1}.

Fig. ES29. Differential Pulsed Voltammograms of Lewis acid adducts in 0.1 M [NBu$_4$][BAr$^F{}_4$] fluorobenzene cooled in a dry ice acetonitrile bath with Fc* (-0.73 V) reference.

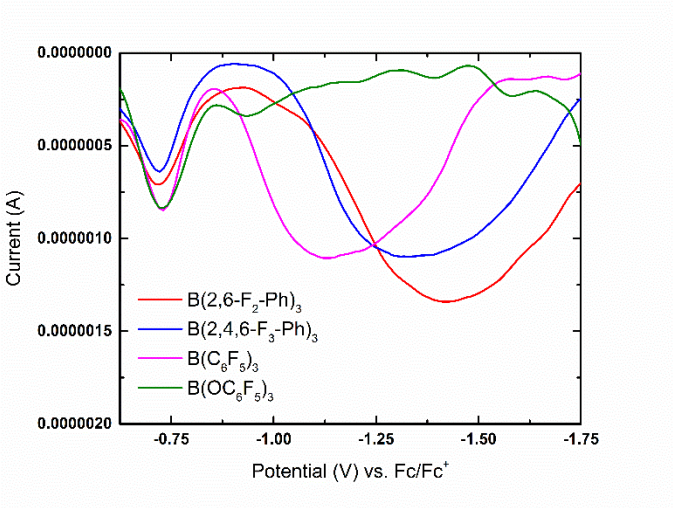

Fig. ES30. Cyclic Voltammogram of 4 in 0.1 M [NBu$_4$][BAr$^F{}_4$] fluorobenzene cooled in a dry ice acetonitrile bath.

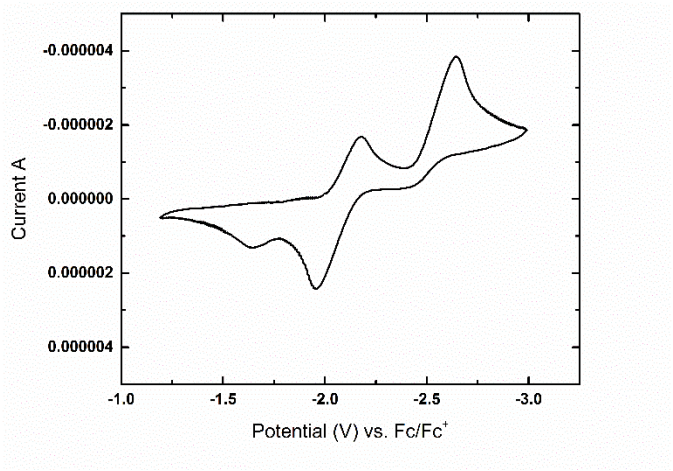

Fig. ES31. Differential Pulsed Voltammogram of 4 in 0.1 M [NBu_4][BAr^F_4] fluorobenzene cooled in a dry ice acetonitrile bath.

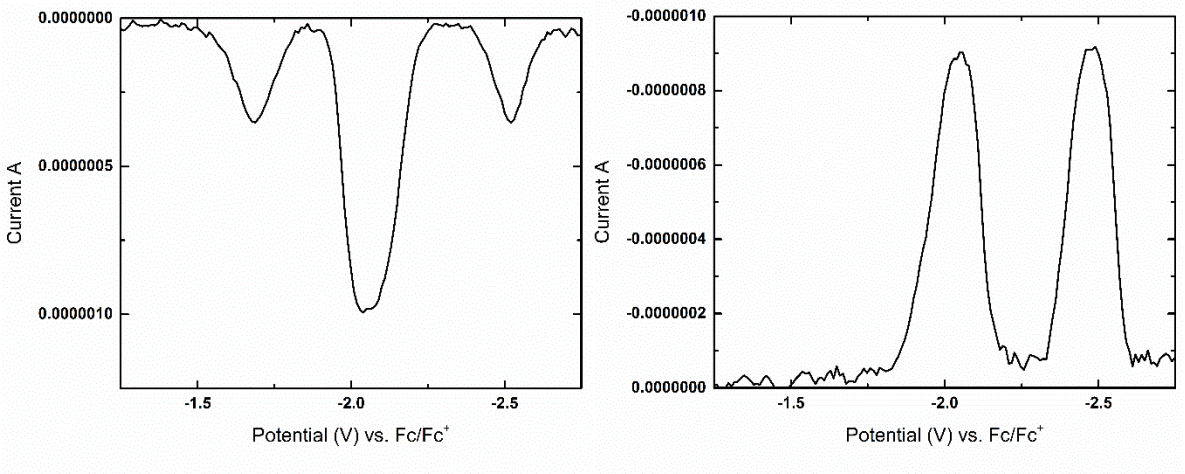

Fig. ES32. Cyclic voltammetry of the reversible oxidation of Fe(II)(^{i}Pr$_2$Tp)Cl in 0.1 M [NBu_4][BAr^F_4] fluorobenzene. No reductive event was observed within the solvent window of fluorobenzene.

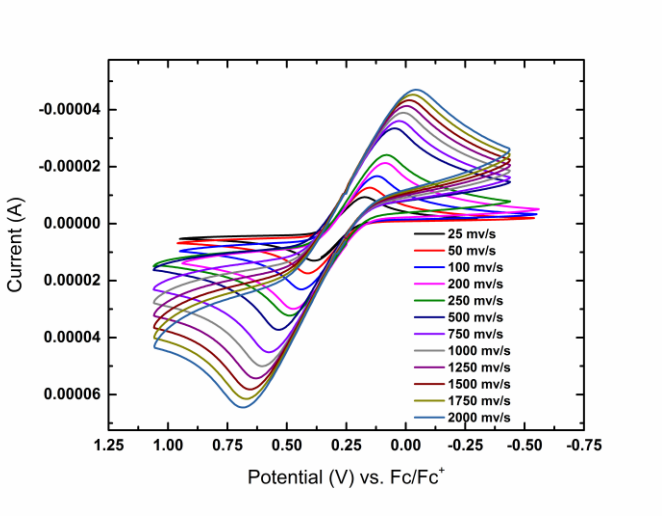

References:

(1) Masami, I.; Hironobu, A.; Hideno, F.; Nobumasa, K.; Yoshihiko, M.-o. *Bulletin of the Chemical Society of Japan* **1996**, *69*, 1937.
(2) Hirano, M.; Akita, M.; Morikita, T.; Kubo, H.; Fukuoka, A.; Komiya, S. *Journal of the Chemical Society, Dalton Transactions* **1997**, 3453.
(3) Yakelis, N. A.; Bergman, R. G. *Organometallics* **2005**, *24*, 3579.
(4) Mon, I.; Jose, D. A.; Vidal-Ferran, A. *Chemistry – A European Journal* **2013**, *19*, 2720.
(5) Brookhart, M.; Grant, B.; Volpe, A. F. *Organometallics* **1992**, *11*, 3920.
(6) Nicasio, J. A.; Steinberg, S.; Inés, B.; Alcarazo, M. *Chemistry – A European Journal* **2013**, *19*, 11016.

(7) Naumann, D.; Butler, H.; Gnann, R. *Zeitschrift für anorganische und allgemeine Chemie* **1992**, *618*, 74.
(8) Ono, T.; Ohta, M.; Sada, K. *ACS Macro Letters* **2012**, *1*, 1270.
(9) Dolomanov, O. V.; Bourhis, L. J.; Gildea, R. J.; Howard, J. A. K.; Puschmann, H. *Journal of Applied Crystallography* **2009**, *42*, 339.
(10) Sheldrick, G. *Acta Crystallographica Section A* **2008**, *64*, 112.